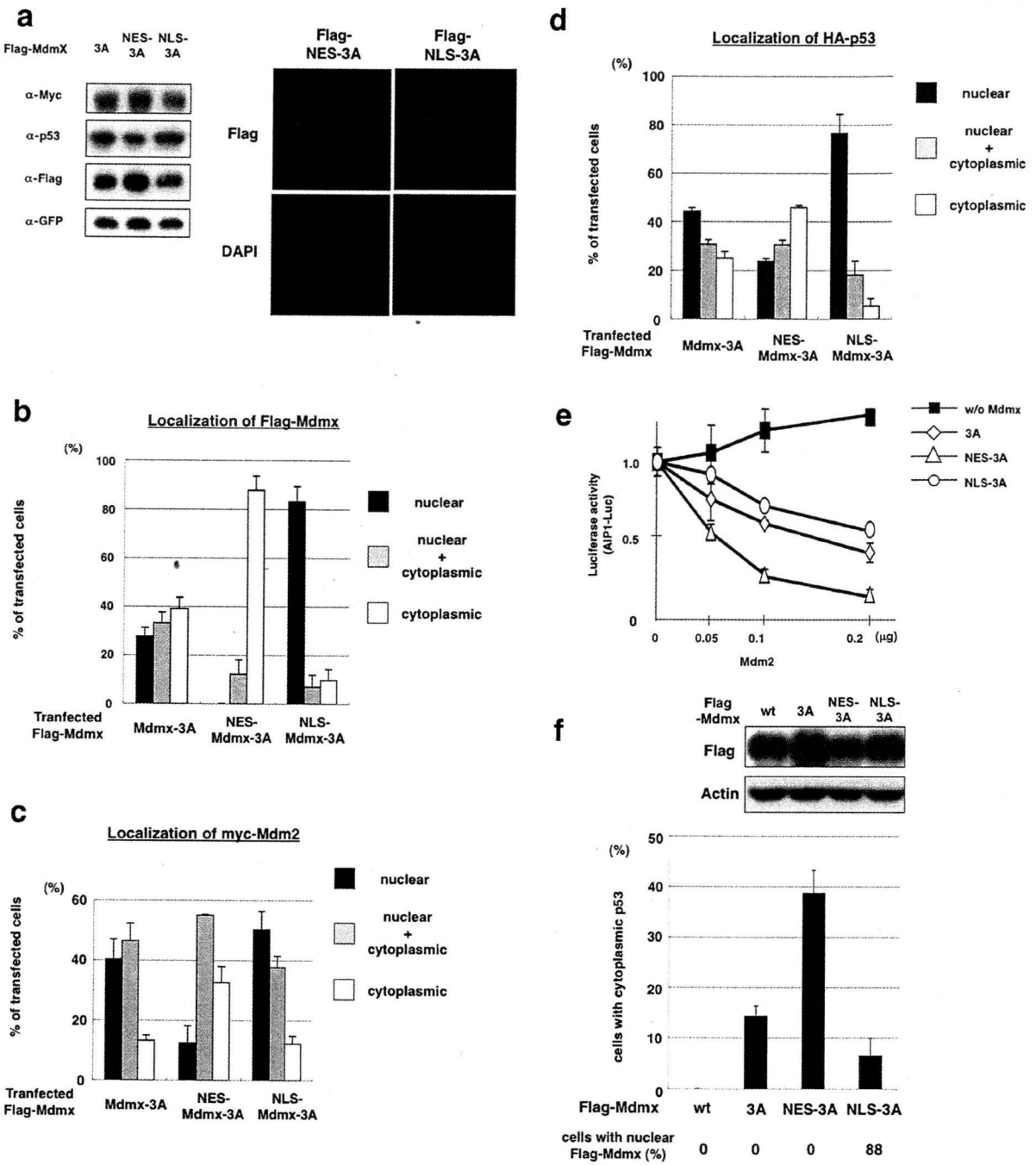

Fig. 4. Cytoplasmic Mdmx tethers p53 and Mdm2 to the cytoplasm and stimulates p53 inhibition. (a) H1299 cells were cotransfected with HA-p53, myc-Mdm2, GFP, and the indicated Flag-tagged Mdmx. Left panel, western blot analyses with the indicated antibodies. Right panel, representative staining with anti-Flag antibody and DAPI. (b–d) H1299 cells were transfected with the indicated Mdmx, together with myc-Mdm2, and immunostained with (b) anti-Flag antibody, (c) anti-Mdm2 antibody, or (d) anti-HA antibody. Subcellular localization of transfected (b) Mdmx, (c) Mdm2, or (d) p53 was represented as described in Figure 2(b). (e) Flag-Mdmx mutant or the control vector was transfected into H1299 cells together with HA-p53, in the presence of the indicated amounts of myc-Mdm2, and luciferase assays were carried out as described in Figure 1(c). (f) U2OS cells were transfected with the indicated Flag-Mdmx. Upper panel, western blot analyses with the anti-Flag or the anti-actin antibodies. Lower panel, cells transfected with the indicated plasmids were immunostained with the anti-Flag and antip53 (CM1) antibodies, and a fraction of the transfected cells with cytoplasmic p53 staining was quantified.

in neuroblastoma cells, we inhibited Mdmx expression by infecting cells with the lentiviruses expressing Mdmx shRNA. Mdmx inhibition by the specific shRNA, while not significantly affecting levels of p53, induced expression of p21, a crucial p53 target (Fig. 5c) and reduced the cytoplasmic localization of p53 (Fig. 5d,e). The positive role of Mdmx in cytoplasmic localization of p53 was confirmed by western blot analyses of nuclear and cytoplasmic lysates prepared from the infected cells. Depletion of Mdmx

doi: 10.1111/j.1349-7006.2009.01180.x

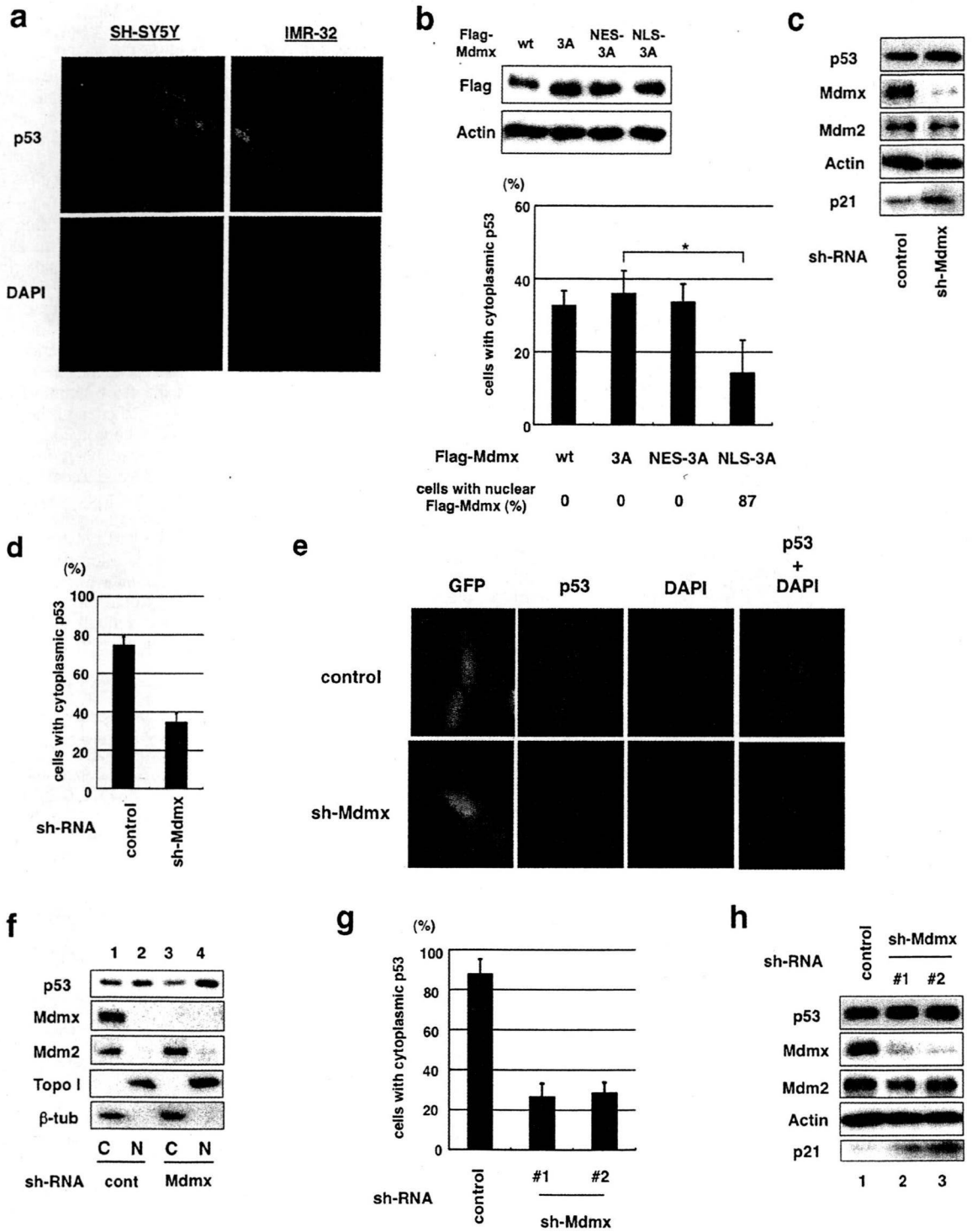

Fig. 5. Mdmx is required for cytoplasmic retention of p53 in neuroblastoma cells. (a) Cytoplasmic retention of p53 in neuroblastoma. SH-SY5Y or IMR-32 cells were stained with antip53 antibody (CM1) and DAPI. (b) SH-SY5Y cells were transfected with the indicated Flag-tagged Mdmx. Western blot analyses and quantification of a fraction of cells with cytoplasmic p53 were carried out as described in Figure 4(f). (c–f) SH-SY5Y cells were infected with the control lentivirus or the viruses expressing Mdmx shRNA. (c) Lysates prepared from the infected cells were used for western blot analyses with the indicated antibodies. (d) The infected cells were immunostained with antip53 polyclonal antibody (CM1) and DAPI. The average percentage of the infected cells with cytoplasmic staining of p53 was presented after evaluating subcellular localization of p53 of 100 cells in triplicate. (e) Representative pictures of staining of cells that were infected with the control lentiviruses or the viruses that express Mdmx shRNA. Note that the viruses express GFP, and infection efficiency is ~100% judging from GFP expression. (f) Subcellular fractionation and western blot analyses were carried out with the indicated antibodies. (g,h) IMR-32 cells were infected with the control lentiviruses or the viruses that express Mdmx shRNA, and (g) western blot analyses or (h) the quantification of subcellular distribution of p53 was carried out as described in (c) and (d) respectively.

decreased p53 levels in the cytoplasm and increased those in nuclei, while the depletion did not significantly affect cytoplasmic localization of Mdm2 (Fig. 5f).

Similarly, inhibition of Mdmx by the specific shRNA led to induction of p21 expression and inhibition of cytoplasmic localization of p53 in IMR-32, another neuroblastoma cell line (Fig. 5g,h; Supporting Information Fig. S4c). Thus, Mdmx contributes to cytoplasmic retention of p53 in neuroblastoma cells.

Discussion

Genetic evidence indicates that *mdmx* is a crucial inhibitor of p53 and that *mdmx* and *mdm2* cooperatively function to inhibit p53. However, the mechanical basis of the cooperation of the oncogenes is not clearly established. In an attempt to recapitulate synergistic inhibition of p53 by Mdmx and Mdm2, we took advantage of our observation that the nonphosphorylatable mutations confer Mdmx resistance against Mdm2-mediated degradation. We demonstrated that nonphosphorylatable mutations of Mdmx markedly enhance the ability of Mdmx to cooperate with Mdm2 for inhibition of p53, suggesting that the stress-induced phosphorylation of Mdmx is important for its ability to suppress p53. The importance of the Mdmx phosphorylation was further supported by the functionality of wild-type Mdmx on p53 suppression in the presence of a chk2 inhibitor (Supporting Information Figs S1b and 2b).

Through the analyses of the function of the Mdmx mutants, we found that the nonphosphorylatable mutant of Mdmx effectively cooperates with Mdm2 to induce p53 ubiquitination. The ability of the nonphosphorylatable mutations of Mdmx to inhibit p53 activity was associated with enhanced cytoplasmic retention of p53 and with increased levels of the interaction of Mdmx to p53 and Mdm2 in cytoplasm. A causal role of cytoplasmic Mdmx to induce localization of p53 in the cytoplasm was demonstrated using the Mdmx mutants that harbor autonomous subcellular localization signals.

p53 is sequestered in the cytoplasm in some types of cancer, and it is assumed that the sequestration of p53 contributes to p53 inactivation.[35,39] Mdm2 is essential for inhibition and cytoplasmic sequestration of p53 in neuroblastoma cells,[36,37] and the cooperative function of Mdmx and Mdm2 to induce p53 retention in the cytoplasm may contribute to its inactivation in some of cancer cells. We found that, in addition to Mdm2, Mdmx is also required for cytoplasmic sequestration of p53 in neuroblastoma cells. Considering that Mdm2 enhances the interaction between p53 and Mdmx in the transfected H1299 cells, Mdmx and Mdm2 may cooperate by stimulating the formation of a complex with p53. Of note, Mdmx stabilizes p53 via a formation of a complex with Mdm2,[16] and formation of such a stable complex may account for cytoplasmic sequestration of p53.

In addition to the cytoplasmic tethering via physical interaction, regulation of post-translational modification of the C-terminal of p53 is likely to contribute to the cooperative inhibition of p53 by Mdm2 and Mdmx, because mutations in the six C-terminal lysines, which are targets for the regulatory modification, partly abolished the cooperative inhibition of p53 (Supporting Information Fig. S2d). Mdm2 promotes cytoplasmic translocation of p53 via its ubiquitination at the same lysine residues,[27,40] and accumulating data[9,18,19] as well as ours (Supporting Information Fig. 2c) indicate that Mdmx promotes Mdm2-dependent p53 ubiquitination. Hence, it is likely that enhancement of Mdm2-dependent ubiquitination of p53 by Mdmx also contributes to the cooperative inhibition of p53 activity by these oncoproteins. In fact, the cytoplasmic retention of p53 in neuroblastoma is in part attributed to multimono-ubiquitination of p53 due to defective function of HAUSP, a de-ubiquitinating enzyme for p53 and Mdmx and Mdm2.[34,41,42] However, we did not observe a significant change in the pattern of p53 laddering, which presumably represents ubiquitinated p53, in neuroblastoma cells after knock down of Mdmx (data not shown). The two mechanisms that mediate cytoplasmic localization of p53, namely cytoplasmic tethering and ubiquitin-dependent translocation, are not mutually exclusive, and presumably contribute to cytoplasmic retention of p53 by Mdmx.

Acknowledgments

We are indebted to Jiandong Chen and Hirofumi Arakawa for providing us with Flag-Mdm2 and AIP-luc respectively. We thank Kenji Kashima for experimental assistance. This work was supported by a Grant-in-Aid for Scientific Research from the Ministry of Education, Culture, Sports, Science, and Technology of Japan (Y.T. and K.O.), a Grant-in-Aid for Third Term Comprehensive Control Research for Cancer from the Ministry of Health, Labor, and Welfare, Japan (Y.T.), the Foundation for Promotion of Cancer Research (K.O.), and the Japan–France Integrated Action Program (K.O. and C.G.).

References

1 Braithwaite AW, Prives CL. p53: more research and more questions. *Cell Death Differ* 2006; **13**: 877–80.
2 Levine AJ. p53, the cellular gatekeeper for growth and division. *Cell* 1997; **88**: 323–31.
3 Oren M. Decision making by p53: life, death and cancer. *Cell Death Differ* 2003; **10**: 431–42.
4 Ko LJ, Prives C. p53: puzzle and paradigm. *Genes Dev* 1996; **10**: 1054–72.
5 Vogelstein B, Lane D, Levine AJ. Surfing the p53 network. *Nature* 2000; **408**: 307–10.
6 Toledo F, Wahl GM. MDM2 and MDM4: p53 regulators as targets in anticancer therapy. *Int J Biochem Cell Biol* 2007; **39**: 1476–8.
7 Marine JC, Dyer MA, Jochemsen AG. MDMX: from bench to bedside. *J Cell Sci* 2007; **120**: 371–8.
8 Marine JC, Francoz S, Maetens M, Wahl G, Toledo F, Lozano G. Keeping p53 in check: essential and synergistic functions of Mdm2 and Mdm4. *Cell Death Differ* 2006; **13**: 927–34.
9 Linares LK, Hengstermann A, Ciechanover A, Muller S, Scheffner M. HdmX stimulates Hdm2-mediated ubiquitination and degradation of p53. *Proc Natl Acad Sci USA* 2003; **100**: 12 009–14.
10 Gu J, Kawai H, Nie L *et al.* Mutual dependence of MDM2 and MDMX in their functional inactivation of p53. *J Biol Chem* 2002; **277**: 19 251–4.
11 Tanimura S, Ohtsuka S, Mitsui K, Shirouzu K, Yoshimura A, Ohtsubo M. MDM2 interacts with MDMX through their RING finger domains. *FEBS Lett* 1999; **447**: 5–9.
12 Sharp DA, Kratowicz SA, Sank MJ, George DL. Stabilization of the MDM2 oncoprotein by interaction with the structurally related MDMX protein. *J Biol Chem* 1999; **274**: 38 189–96.
13 Michael D, Oren M. The p53–Mdm2 module and the ubiquitin system. *Semin Cancer Biol* 2003; **13**: 49–58.
14 Honda R, Tanaka H, Yasuda H. Oncoprotein MDM2 is a ubiquitin ligase E3 for tumor suppressor p53. *FEBS Lett* 1997; **420**: 25–7.
15 Coutts AS, La Thangue NB. Mdm2 widens its repertoire. *Cell Cycle* 2007; **6**: 827–9.
16 Stad R, Little NA, Xirodimas DP *et al.* Mdmx stabilizes p53 and Mdm2 via two distinct mechanisms. *EMBO Rep* 2001; **2**: 1029–34.
17 Toledo F, Krummel KA, Lee CJ *et al.* A mouse p53 mutant lacking the proline-rich domain rescues Mdm4 deficiency and provides insight into the Mdm2-Mdm4-p53 regulatory network. *Cancer Cell* 2006; **9**: 273–85.
18 Poyurovsky MV, Priest C, Kentsis A *et al.* The Mdm2 RING domain C-terminus is required for supramolecular assembly and ubiquitin ligase activity. *EMBO J* 2007; **26**: 90–101.
19 Uldrijan S, Pannekoek WJ, Vousden KH. An essential function of the extreme C-terminus of MDM2 can be provided by MDMX. *EMBO J* 2007; **26**: 102–12.
20 Shinozaki T, Nota A, Taya Y, Okamoto K. Functional role of Mdm2 phosphorylation by ATR in attenuation of p53 nuclear export. *Oncogene* 2003; **22**: 8870–80.
21 Laurie NA, Donovan SL, Shih CS *et al.* Inactivation of the p53 pathway in retinoblastoma. *Nature* 2006; **444**: 61–6.
22 Pereg Y, Shkedy D, de Graaf P *et al.* Phosphorylation of Hdmx mediates its Hdm2- and ATM-dependent degradation in response to DNA damage. *Proc Natl Acad Sci USA* 2005; **102**: 5056–61.

doi: 10.1111/j.1349-7006.2009.01180.x

23 Okamoto K, Kashima K, Pereg Y *et al.* DNA damage-induced phosphorylation of MdmX at serine 367 activates p53 by targeting MdmX for Mdm2-dependent degradation. *Mol Cell Biol* 2005; **25**: 9608–20.
24 Jin Y, Dai MS, Lu SZ *et al.* 14-3-3gamma binds to MDMX that is phosphorylated by UV-activated Chk1, resulting in p53 activation. *EMBO J* 2006; **25**: 1207–18.
25 Pereg Y, Lam S, Teunisse A *et al.* Differential roles of ATM- and Chk2-mediated phosphorylations of Hdmx in response to DNA damage: *Mol Cell Biol* 2006; **26**: 6819–31.
26 Chen L, Gilkes DM, Pan Y, Lane WS, Chen J. ATM and Chk2-dependent phosphorylation of MDMX contribute to p53 activation after DNA damage. *EMBO J* 2005; **24**: 3411–22.
27 Shmueli A, Oren M. Regulation of p53 by Mdm2: fate is in the numbers. *Mol Cell* 2004; **13**: 4–5.
28 Lopez-Pajares V, Kim MM, Yuan ZM. Phosphorylation of MDMX mediated by Akt leads to stabilization and induces 14-3-3 binding. *J Biol Chem* 2008; **283**: 13707–13.
29 Gu J, Nie L, Wiederschain D, Yuan ZM. Identification of p53 sequence elements that are required for MDM2-mediated nuclear export. *Mol Cell Biol* 2001; **21**: 8533–46.
30 Lohrum MA, Woods DB, Ludwig RL, Balint E, Vousden KH. C-terminal ubiquitination of p53 contributes to nuclear export. *Mol Cell Biol* 2001; **21**: 8521–32.
31 Xirodimas DP, Saville MK, Bourdon JC, Hay RT, Lane DP. Mdm2-mediated NEDD8 conjugation of p53 inhibits its transcriptional activity. *Cell* 2004; **118**: 83–97.
32 Toledo F, Wahl GM. Regulating the p53 pathway: *in vitro* hypotheses, *in vivo* veritas. *Nat Rev Cancer* 2006; **6**: 909–23.
33 Singh RK, Iyappan S, Scheffner M. Hetero-oligomerization with MdmX rescues the ubiquitin/Nedd8 ligase activity of RING finger mutants of Mdm2. *J Biol Chem* 2007; **282**: 10 901–7.
34 Becker K, Marchenko ND, Maurice M, Moll UM. Hyperubiquitylation of wild-type p53 contributes to cytoplasmic sequestration in neuroblastoma. *Cell Death Differ* 2007; **14**: 1350–60.
35 Moll UM, LaQuaglia M, Benard J, Riou G. Wild-type p53 protein undergoes cytoplasmic sequestration in undifferentiated neuroblastomas but not in differentiated tumors. *Proc Natl Acad Sci USA* 1995; **92**: 4407–11.
36 Lu W, Pochampally R, Chen L, Traidej M, Wang Y, Chen J. Nuclear exclusion of p53 in a subset of tumors requires MDM2 function. *Oncogene* 2000; **19**: 232–40.
37 Rodriguez-Lopez AM, Xenaki D, Eden TO, Hickman JA, Chresta CM. MDM2 mediated nuclear exclusion of p53 attenuates etoposide-induced apoptosis in neuroblastoma cells. *Mol Pharmacol* 2001; **59**: 135–43.
38 Danovi D, Meulmeester E, Pasini D *et al.* Amplification of Mdmx (or Mdm4) directly contributes to tumor formation by inhibiting p53 tumor suppressor activity. *Mol Cell Biol* 2004; **24**: 5835–43.
39 Jimenez GS, Khan SH, Stommel JM, Wahl GM. p53 regulation by post-translational modification and nuclear retention in response to diverse stresses. *Oncogene* 1999; **18**: 7656–65.
40 Li M, Brooks CL, Wu-Baer F, Chen D, Baer R, Gu W. Mono-versus polyubiquitination: differential control of p53 fate by Mdm2. *Science* 2003; **302**: 1972–5.
41 Li M, Brooks CL, Kon N, Gu W. A dynamic role of HAUSP in the p53–Mdm2 pathway. *Mol Cell* 2004; **13**: 879–86.
42 Meulmeester E, Maurice MM, Boutell C *et al.* Loss of HAUSP-mediated deubiquitination contributes to DNA damage-induced destabilization of Hdmx and Hdm2. *Mol Cell* 2005; **18**: 565–76.

Supporting Information

Additional Supporting Information may be found in the online version of this article:

Supporting Information Materials and Methods

Fig. S1. Non-phosphorylatable Mdmx cooperates with Mdm2 to suppress p53.

Fig. S2. Non-phosphorylatable Mdmx cooperates with Mdm2 to induce cytoplasmic localization of p53 in H1299.

Fig. S3. The Mdmx-3A mutation stimulates the localization of Mdm2 and p53 predominantly to the cytoplasm.

Fig. S4. Mdmx is required for cytoplasmic retention of p53 in neuroblastoma cells.

Please note: Wiley-Blackwell are not responsible for the content or functionality of any supporting materials supplied by the authors. Any queries (other than missing material) should be directed to the corresponding author for the article.

Adiponectin inhibits colorectal cancer cell growth through the AMPK/mTOR pathway

MICHIKO SUGIYAMA[1], HIROKAZU TAKAHASHI[1], KUNIHIRO HOSONO[1], HIROKI ENDO[1], SHINGO KATO[1], KYOKO YONEDA[1], YUICHI NOZAKI[1], KOJI FUJITA[1], MASATO YONEDA[1], KOICHIRO WADA[2], HITOSHI NAKAGAMA[3] and ATSUSHI NAKAJIMA[1]

[1]Division of Gastroenterology, Yokohama City University School of Medicine, 3-9 Fuku-ura, Kanazawa-ku, Yokohama; [2]Department of Pharmacology, Graduate School of Dentistry, Osaka University, 1-8 Yamadaoka, Suita, Osaka; [3]Biochemistry Division, National Cancer Center Research Institute, 1-1 Tsukiji 5-chome, Chuo-ku, Tokyo, Japan

Received July 2, 2008; Accepted September 25, 2008

DOI: 10.3892/ijo_00000156

Abstract. Adiponectin is a peptide hormone secreted by adipose tissue. It is a key hormone responsible for insulin sensitization, and its circulating level is inversely associated with abdominal obesity. Recent studies have shown that a reduced plasma adiponectin level is significantly correlated with the risk of various cancers. However, there are few studies regarding the association of adiponectin and colorectal cancer. To address this issue, we investigated the effect of adiponectin on colorectal cancer cells. Three colorectal cancer cell lines express both AdipoR1 and AdipoR2 receptors. MTT assay revealed that adiponectin inhibited human colorectal cancer cell growth. Furthermore, Western blot analysis revealed that adiponectin activated adenosine monophosphate-activated protein kinase (AMPK) and suppressed mammalian target of rapamycin (mTOR) pathways. Selective AMPK inhibitor compound C abrogated the inhibitory effect of adiponectin on cell growth. Our results clearly demonstrate the novel findings that adiponectin inhibits colorectal cancer cell growth via activation of AMPK, thereby down-regulating the mTOR pathway.

Introduction

Colorectal cancer (CRC) is one of the most common malignancies. Obesity, especially visceral obesity, has been reported to be associated with CRC (1,2). Adipose tissue is not only a fat storage organ, but it secretes several bioactive substances known as adipocytokines (3,4). Adiponectin is secreted from adipocytes and is a key hormone responsible for insulin sensitization (5-12). Its plasma level is dramatically decreased in patients with obesity and type 2 diabetes mellitus (DM) (4,5,13). Since both obesity and type 2 DM have been reported to be associated with an elevated risk of CRC (14), it is speculated that the plasma level of adiponectin may be related to the risk of CRC. However, several contradictory results have been reported from human clinical studies on the relationship between the plasma levels of adiponectin and the risk of CRC (15,16).

It is well known that the adiponectin receptor exists in two isoforms: adiponectin receptor 1 (AdipoR1) and 2 (AdipoR2) (17). These receptors mediate cellular functions by activating intracellular signaling pathways (17). The molecular pathways downstream of AdipoRs remain to be fully elucidated, but studies in metabolically-responsive cells have shown that activation of the pleiotropic adenosine monophosphate-activated protein kinase (AMPK) is involved in the signaling cascade downstream of adiponectin receptors (18,19). AMPK plays a key role in the regulation of energy homeostasis and acts as a 'metabolic sensor' to regulate adenosine triphosphate (ATP) concentrations (20). It is also associated with cell growth; phosphorylated AMPK suppresses mammalian target of rapamycin (mTOR) signaling pathway (21,22). mTOR plays a central role in the regulation of cell proliferation, growth, differentiation, migration and survival (23-26), and may be abnormally regulated in tumors (23,27-29). The 70-kDa ribosomal protein S6 kinase (p70S6K) and S6 ribosomal protein (S6P) are part of the signaling cascade downstream of mTOR; they are activated via phosphorylation by mTOR (28,30,31). Non-cleaved adiponectin (full-length adiponectin; f-adiponectin) and proteolytically-cleaved adiponectin containing a C-terminal globular region (globular adiponectin; g-adiponectin) were reported to have different affinities to AdipoR1 and AdipoR2 (17). In this study, we only examined the g-adiponectin because this isoform binds both receptors, while f-adiponectin has low affinity to AdipoR1 (17), and it exerts more potent effect than f-adiponectin (5). However, the expression levels of AdipoR1 and AdipoR2, the affinity of the different forms of

Correspondence to: Dr Atsushi Nakajima, Division of Gastroenterology, Yokohama City University School of Medicine, 3-9 Fuku-ura, Kanazawa-ku, Yokohama, Japan
E-mail: nakajima-tky@umin.ac.jp

Key words: adiponectin, colorectal cancer, cell growth, AdipoR1/AdipoR2, adenosine monophosphate-activated protein kinase

adiponectin to those receptors, and the associated intracellular signaling pathways in the colorectum remain unclear. In this study, we investigated the effect of adiponectin on cell growth and the intracellular signaling pathway involved in CRC cell lines.

Materials and methods

Reagents and antibodies. Human globular adiponectin was purchased from BioVendor Laboratory Medicine Inc. (Brno, Czech Republic). Compound C was purchased from Calbiochem (La Jolla, CA) and 3-(4,5-dimethyl-thiazol-2-yl)-2,5-diphenyl tetrazolium bromide (MTT) was purchased from Sigma Chemical Co. (St. Louis, MO). Anti-total and -phosphorylated (Thr172) AMPK, anti-total and -phosphorylated (Ser2448) mTOR, anti-total and -phosphorylated (Thr421/Ser424) p70S6 kinase, anti-total and -phosphorylated (Ser240/244) S6 ribosomal protein, and anti-rabbit horseradish-peroxidase-conjugated IgG antibodies were obtained from Cell Signaling Technology, Inc. (Beverly, MA). Anti-AdipoR1 (C-14), anti-AdipoR2 (N-19), and anti-goat horseradish-peroxidase-conjugated IgG antibodies were from Santa Cruz Biotechnology, Inc. (Santa Cruz, CA). Anti-glyceraldehyde-3-phosphate dehydrogenase (G3PDH) antibody was from Trevigen, Inc. (Gaithersburg, MD).

Cell lines. The human colon adenocarcinoma cell lines, HT-29, Lovo, and HCT116 were used for this study. Lovo was obtained from Health Science Research Resources Bank (Osaka, Japan), while HT-29 and HCT116 were obtained from American Type Culture Collection (Manassas, VA). HCT116 and HT-29 were cultured in McCoy's 5A, and Lovo was cultured in Ham's F12, supplemented with 10% FBS, penicillin (100 U/ml) and streptomycin (100 μg/ml) (all from Invitrogen, Carlsbad, CA) at 37°C under a humidified atmosphere of 5% CO_2.

Western blot analysis. Cultured cells treated with the test compound for indicated time periods were rinsed with phosphate-buffer saline (PBS). For obtaining the total cell extracts, cells were harvested in lysis buffer (50 mM Tris-HCl, 100 mM NaCl, 5 mM EDTA, 1% TritonX-100) containing a cocktail of protease inhibitors (Sigma). The lysates were incubated on ice for 30 min and centrifuged at 15,000 rpm. Protein concentrations were determined using the Bio-Rad Protein Assay Reagent (Bio-Rad, Richmond, CA). Proteins were separated by SDS/PAGE (7.5-12.5% gels) and transferred onto a Hybond-P PVDF membrane (Amersham Biosciences, Little Chalfont, UK). After the transfer, the membranes were blocked with Blocking One-P (Nacalai Tesque, Kyoto, Japan) and probed with the primary antibodies specified below. Horseradish-peroxidase-conjugated secondary antibodies and the ECL detection kit (Amersham Biosciences, Little Chalfont, UK) were used for the detection of specific proteins. Images were captured and analyzed by LAS-3000 imaging system (Fujifilm, Tokyo, Japan).

Cell growth assay. Cells were seeded in 96-well, flat-bottom microtiter plates at a density of $5x10^3$ cells per well and incubated in medium containing 1% FBS. After 24 h, the complete medium was replaced with test medium for 24 h at 37°C. After incubating the plates for an additional 4 h with MTT solution (0.5%), sodium dodecylsulfate was added to a final concentration of 10% and absorbance at 595 nm was determined for each well using a microplate reader (Model 550; Bio-Rad). Three independent experiments were carried out for each cell line. Annexin V-FITC and PI double staining with the Annexin V-FITC apoptosis detection kit I (Becton-Dickinson, San Jose, CA, USA) followed by FACScan flow cytometry (Becton-Dickinson) was used to identify apoptotic cells. Cell fluorescence was measured with a FACScan flow cytometer from BD Biosciences (San Jose, CA, USA). Dual parameter cytometric data were analyzed by using CellQuest software from BD Biosciences. Apoptosis measures were performed in triplicate.

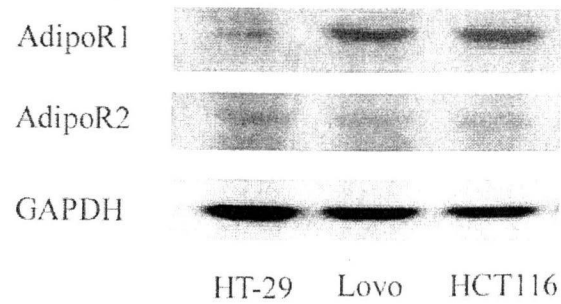

Figure 1. Expression of adiponectin receptors in colorectal cancer cells. Western blot analysis revealed that three kinds of colorectal cancer cell lines HCT116, HT-29 and Lovo cells, expressed both AdipoR1 and AdipoR2 receptors.

Statistical analysis. All results are expressed as mean ± SEM. Statistical analyses were performed using Student's t-test after analysis of variance (ANOVA). The results were considered to be statistically significant at $p<0.05$.

Results

Expression of adiponectin receptors on colorectal cancer cells. Western blot analysis revealed that three kinds of colorectal cancer cell lines, HCT116, HT-29 and Lovo, expressed both AdipoR1 and AdipoR2 receptors (Fig. 1). In HT-29, weak expressions of both of AdipoRs were observed. In Lovo and HCT116, strong expression of AdipoR1, and weak expression of AdipoR2 were observed.

Globular adiponectin (g-adiponectin) inhibited human colorectal cancer cell growth. To determine the effect of g-adiponectin on colorectal cancer cell growth, MTT assay was performed using HCT116, HT-29 and Lovo cells. To reduce the effect of adiponectin in serum, all experiments were conducted using the culture medium containing 1% FBS. G-adiponectin significantly inhibited colorectal cancer cell growth in all examined cells in a dose-dependent manner (Fig. 2).

G-adiponectin up-regulates AMPK activity in colorectal cancer cells. The effect of g-adiponectin on the phosphorylation of

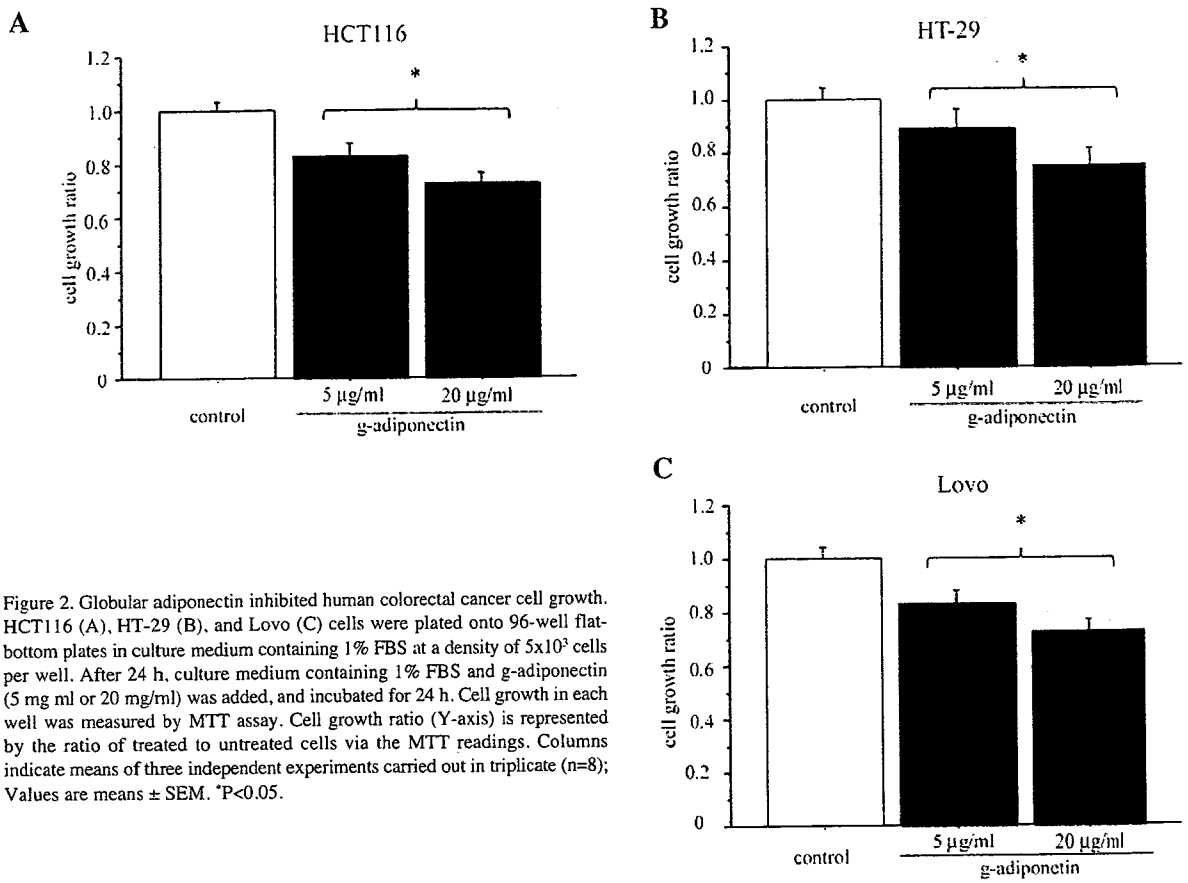

Figure 2. Globular adiponectin inhibited human colorectal cancer cell growth. HCT116 (A), HT-29 (B), and Lovo (C) cells were plated onto 96-well flat-bottom plates in culture medium containing 1% FBS at a density of $5x10^3$ cells per well. After 24 h, culture medium containing 1% FBS and g-adiponectin (5 mg ml or 20 mg/ml) was added, and incubated for 24 h. Cell growth in each well was measured by MTT assay. Cell growth ratio (Y-axis) is represented by the ratio of treated to untreated cells via the MTT readings. Columns indicate means of three independent experiments carried out in triplicate (n=8); Values are means ± SEM. *P<0.05.

AMPK and mTOR signaling pathway was examined. Western blot analysis revealed that g-adiponectin significantly phosphorylated AMPK and its effect on AMPK phosphorylation was maximal at 6 h after treatment (Fig. 3A). We also observed the significant phosphorylation of mTOR, p70S6K, and S6 proteins by the treatment with g-adiponectin (Fig. 3B-D). These results suggest that g-adiponectin inhibits colorectal cancer cell growth via AMPK activation and mTOR signaling pathway suppression. Selective AMPK inhibitor compound C reversed the g-adiponectin induced cell growth inhibition in HCT116 colorectal cancer cells, as detected by MTT assay (Fig. 3E). This indicates that g-adiponectin-induced cell growth inhibition is mediated by activation of AMPK.

G-adiponectin has no effect on apoptosis. The effect of g-adiponectin on apoptosis in HCT116 and HT-29 was evaluated using annexin V-FITC and PI double staining. There was no apoptotic effect in HCT116 and HT-29 treated with 5 μg/ml g-adiponectin or 20 μg/ml g-adiponectin in basal medium containing 1% FBS (Fig. 4).

Discussion

The association of low plasma adiponectin level and cancer risk was previously reported (32-35). However, there are few studies regarding the association of adiponectin and colorectal cancer (15,36). In the present study, we demonstrated both of the AdipoR expression levels and g-adiponectin activation of the AMPK, resulting in the suppression of mTOR signaling pathway in colorectal cancer cell lines. Our recent study demonstrated that AdipoRs were expressed in normal colon epithelial and colorectal cancer cells in human (37). In this study, three kinds of colorectal cancer cell lines HCT116, HT-29 and Lovo cells were shown to express AdipoRs. Furthermore, we clearly demonstrated that globular adiponectin inhibited colorectal cancer cell growth and activated AMPK, while selective AMPK inhibitor compound C reversed the effect of g-adiponectin-induced cell growth inhibition, which indicates that g-adiponectin inhibits cell growth via regulation of AMPK. mTOR is one of the enzymes downstream of AMPK. AMPK activation acts as an inhibitor of mTOR pathway and suppresses tumor development (38,39). In this study, we demonstrated that g-adiponectin suppressed the mTOR pathway following the activation of AMPK. These results suggest that g-adiponectin suppresses cancer cell growth through AMPK activation and subsequent inhibition of mTOR pathway. However, the mechanisms through which adiponectin affects cancer cells are not completely elucidated, thus there is a possibility that suppression of mTOR pathway by adiponectin is mediated through other enzymes (40,41). Further studies are needed to evaluate the molecular pathways downstream of each AdipoR.

In conclusion, this study clearly demonstrates the novel findings that g-adiponectin inhibits colorectal cancer cell

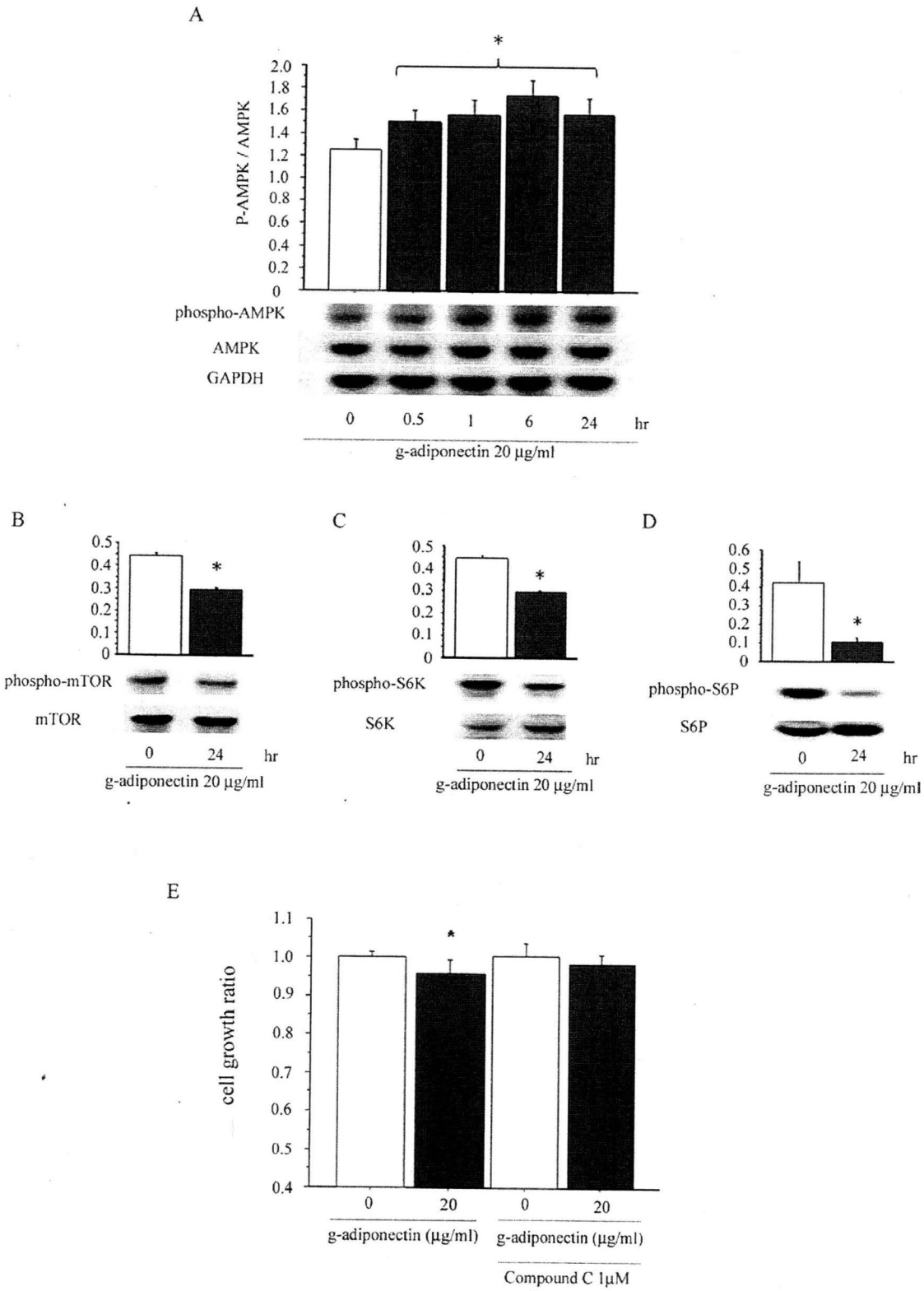

Figure 3. G-adiponectin up-regulates AMPK activity in colorectal cancer cell and selective AMPK inhibitor compound C reversed the g-adiponectin-induced cell growth. Western blot analysis was performed. HCT116 cells were treated with culture medium containing 1% FBS and g-adiponectin (20 μg/ml) for 24 h. After harvesting, cells were lysed and prepared for immunoblot analysis. (A) G-adiponectin increases AMPK phosphorylation and its effect on AMPK phosphorylation was maximal at 6 h after treatment. (B-D) G-adiponectin reduced phosphorylation of mTOR, p70S6K and S6P in HCT116 cells. Western blot analysis was performed in triplicate. Values are means ± SEM. *P<0.05. (E) To confirm the effect of adiponectin-induced growth inhibition via AMPK, HCT116 incubated in culture medium containing 1% FBS and adiponectin (20 μg/ml) alone or with the addition of compound C (1 μM) for 24 h were used for MTT assay. Columns indicate means of four independent experiments carried out in triplicate (n=8); Values are means ± SEM. *P<0.05.

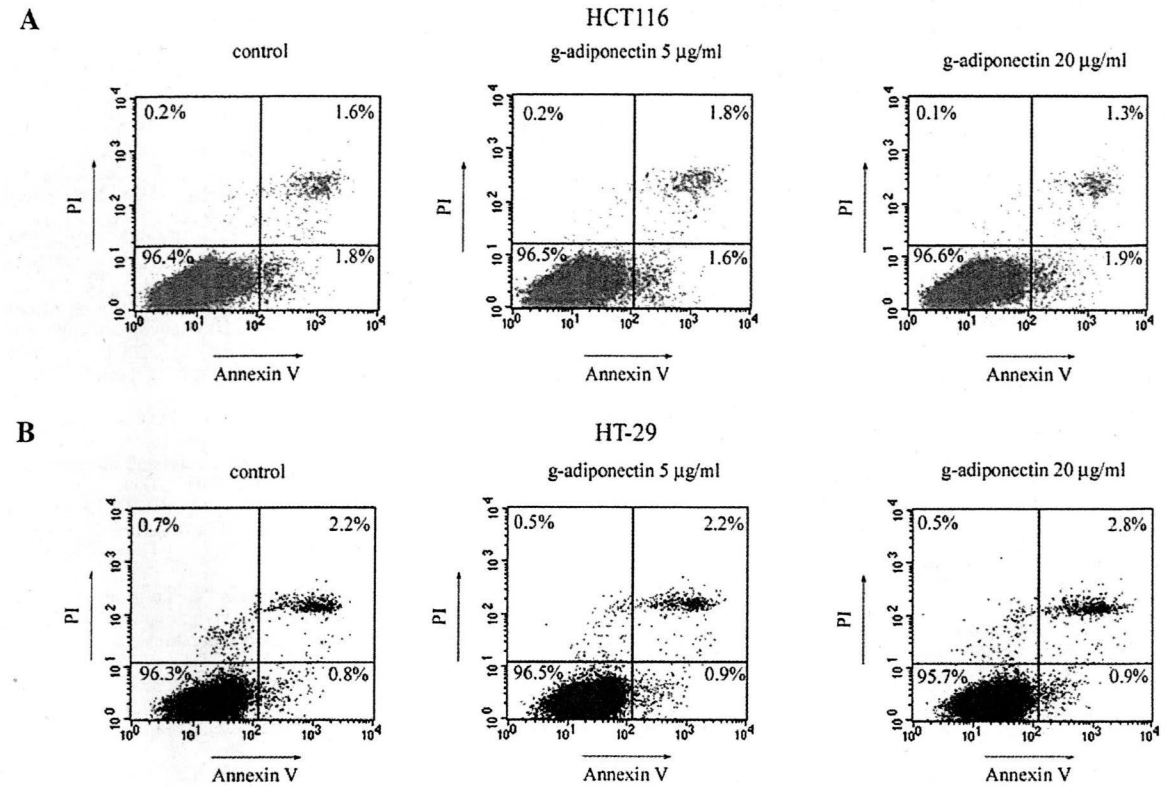

Figure 4. G-adiponectin has no effect on apoptosis. The apoptotic effect of g-adiponectin in HCT116 (A) and HT-29 (B) colorectal cancer cells incubated with culture medium containing 1% FBS and g-adiponectin (5 μg/ml or 20 μg/ml) were evaluated via annexin V-FITC and PI double staining. Apoptosis measures were performed in triplicate.

growth through the activation of AMPK and subsequent suppression of mTOR pathway. This may be a key step in the elucidation of the effect of adiponectin on colorectal cancer. Further studies are required to elucidate the function of adiponectin in colorectal cancer.

Acknowledgements

We thank Machiko Hiraga and Yuko Sato for their technical assistance. This work was supported in part by a Grant-in-Aid for research on the Third Term Comprehensive Control Research for Cancer from the Ministry of Health, Labour and Welfare, Japan to A.N., a grant from the National Institute of Biomedical Innovation (NBIO) to A.N., a grant from the Ministry of Education, Culture, Sports, Science and Technology, Japan (KIBAN-B) to A.N, and a research grant from the Princess Takamatsu Cancer Research Fund to A.N.

References

1. Pischon T, Lahmann PH, Boeing H, Friedenreich C, Norat T, Tjønneland A, Halkjaer J, Overvad K, Clavel-Chapelon F, Boutron-Ruault MC, Guernec G, Bergmann MM, Linseisen J, Becker N, Trichopoulou A, Trichopoulos D, Sieri S, Palli D, Tumino R, Vineis P, Panico S, Peeters PH, Bueno-de-Mesquita HB, Boshuizen HC, van Guelpen B, Palmqvist R, Berglund G, Gonzalez CA, Dorronsoro M, Barricarte A, Navarro C, Martinez C, Quirós JR, Roddam A, Allen N, Bingham S, Khaw KT, Ferrari P, Kaaks R, Slimani N and Riboli E: Body size and risk of colon and rectal cancer in the European Prospective Investigation Into Cancer and Nutrition (EPIC). J Natl Cancer Inst 98: 920-931, 2006.
2. Takahash H, Yoneda K, Tomimoto A, Endo H, Fujisawa T, Iida H, Mawatari H, Nozaki Y, Ikeda T, Akiyama T, Yoneda M, Inamori M, Abe Y, Saito S, Nakajima A and Nakagama H: Life style-related diseases of the digestive system: colorectal cancer as a life style-related disease: from carcinogenesis to medical treatment. J Pharmacol Sci 105: 129-132, 2007.
3. Spranger J, Kroke A, Möhlig M, Bergmann MM, Ristow M, Boeing H and Pfeiffer AF: Adiponectin and protection against type 2 DM. Lancet 361: 226-228, 2003.
4. Hotta K, Funahashi T, Arita Y, Takahashi M, Matsuda M, Okamoto Y, Iwahashi H, Kuriyama H, Ouchi N, Maeda K, Nishida M, Kihara S, Sakai N, Nakajima T, Hasegawa K, Muraguchi M, Ohmoto Y, Nakamura T, Yamashita S, Hanafusa T and Matsuzawa Y: Plasma concentrations of a novel, adipose-specific protein, adiponectin, in type 2 diabetic patients. Arterioscler Thromb Vasc Biol 20: 1595-1599, 2000.
5. Yamauchi T, Kamon J, Waki H, Terauchi Y, Kubota N, Hara K, Mori Y, Ide T, Murakami K, Tsuboyama-Kasaoka N, Ezaki O, Akanuma Y, Gavrilova O, Vinson C, Reitman ML, Kagechika H, Shudo K, Yoda M, Nakano Y, Tobe K, Nagai R, Kimura S, Tomita M, Froguel P and Kadowaki T: The fat-derived hormone adiponectin reverses insulin resistance associated with both lipoatrophy and obesity. Nat Med 7: 941-946, 2001.
6. Berg AH, Combs TP, Du X, Brownlee M and Scherer PE: The adipocyte-secreted protein Acrp30 enhances hepatic insulin action. Nat Med 7: 947-953, 2001.
7. Kubota N, Terauchi Y, Yamauchi T, Kubota T, Moroi M, Matsui J, Eto K, Yamashita T, Kamon J, Satoh H, Yano W, Froguel P, Nagai R, Kimura S, Kadowaki T and Noda T: Disruption of adiponectin causes insulin resistance and neointimal formation. J Biol Chem 277: 25863-25866, 2002.
8. Maeda N, Shimomura I, Kishida K, Nishizawa H, Matsuda M, Nagaretani H, Furuyama N, Kondo H, Takahashi M, Arita Y, Komuro R, Ouchi N, Kihara S, Tochino Y, Okutomi K, Horie M, Takeda S, Aoyama T, Funahashi T and Matsuzawa Y: Diet-induced insulin resistance in mice lacking adiponectin/ACRP30. Nat Med 8: 731-737, 2002.

9. Yamauchi T, Kamon J, Minokoshi Y, Ito Y, Waki H, Uchida S, Yamashita S, Noda M, Kita S, Ueki K, Eto K, Akanuma Y, Froguel P, Foufelle F, Ferre P, Carling D, Kimura S, Nagai R, Kahn BB and Kadowaki T: Adiponectin stimulates glucose utilization and fatty-acid oxidation by activating AMP-activated protein kinase. Nat Med 8: 1288-1295, 2002.
10. Tomas E, Tsao TS, Saha AK, Murrey HE, Zhang Cc C, Itani SI, Lodish HF and Ruderman NB: Enhanced muscle fat oxidation and glucose transport by ACRP30 globular domain: acetyl-CoA carboxylase inhibition and AMP-activated protein kinase activation. Proc Natl Acad Sci USA 99: 16309-16313, 2002.
11. Yamauchi T, Kamon J, Waki H, Imai Y, Shimozawa N, Hioki K, Uchida S, Ito Y, Takakuwa K, Matsui J, Takata M, Eto K, Terauchi Y, Komeda K, Tsunoda M, Murakami K, Ohnishi Y, Naitoh T, Yamamura K, Ueyama Y, Froguel P, Kimura S, Nagai R and Kadowaki T: Globular adiponectin protected ob/ob mice from diabetes and apoE deficient mice from atherosclerosis. J Biol Chem 278: 2461-2468, 2003.
12. Tilg H and Hotamisligil GS: Non-alcoholic fatty liver disease: cytokine-adipokine interplay and regulation of insulin resistance. Gastroenterology 131: 934-945, 2006.
13. Hu E, Liang P and Spiegelman BM: AdipoQ is a novel adipose-specific gene dysregulated in obesity. J Biol Chem 271: 10697-10703, 1996.
14. Giovannucci E and Michaud D: The role of obesity and related metabolic disturbances in cancers of the colon, prostate, and pancreas. Gastroenterology 132: 2208-2225, 2007.
15. Wei EK, Giovannucci E, Fuchs CS, Willett WC and Mantzoros CS: Low plasma adiponectin levels and risk of CRC in men: a prospective study. J Natl Cancer Inst 97: 1688-1694, 2005.
16. Lukanova A, Söderberg S, Kaaks R, Jellum E and Stattin P: Serum adiponectin is not associated with risk of colorectal cancer. Cancer Epidemiol Biomarkers Prev 15: 401-402, 2006.
17. Yamauchi T, Kamon J, Ito Y, Tsuchida A, Yokomizo T, Kita S, Sugiyama T, Miyagishi M, Hara K, Tsunoda M, Murakami K, Ohteki T, Uchida S, Takekawa S, Waki H, Tsuno NH, Shibata Y, Terauchi Y, Froguel P, Tobe K, Koyasu S, Taira K, Kitamura T, Shimizu T, Nagai R and Kadowaki T: Cloning of adiponectin receptors that mediate antidiabetic metabolic effects. Nature 423: 762-769, 2003.
18. Goldstein BJ and Scalia R: Adiponectin: a novel adipokine linking adipocytes and vascular function. J Clin Endocrinol Metab 89: 2563-2568, 2004.
19. Luo Z, Saha AK, Xiang X and Ruderman NB: AMPK, the metabolic syndrome and cancer. Trends Pharmacol Sci 26: 69-76, 2005.
20. Long YC and Zierath JR: AMP-activated protein kinase signaling in metabolic regulation. J Clin Invest 116: 1776-1783, 2006.
21. Bolster DR, Crozier SJ, Kimball SR and Jefferson LS: AMP-activated protein kinase suppresses protein synthesis in rat skeletal muscle through downregulated mTOR signaling. J Biol Chem 277: 23977-23980, 2002.
22. Krause U, Bertrand L and Hue L: Control of p70 ribosomal protein S6 kinase and acetyl-CoA carboxylase by AMP-activated protein kinase and protein phosphatases in isolated hepatocytes. Eur J Biochem 269: 3751-3759, 2002.
23. Vogt PK: PI 3-kinase, mTOR, protein synthesis and cancer. Trends Mol Med 7: 482-484, 2001.
24. Valentinis B and Baserga R: IGF-I receptor signalling in transformation and differentiation. Mol Pathol 54: 133-137, 2001.
25. Oldham S and Hafen E: Insulin/IGF and target of rapamycin signaling: a TOR de force in growth control. Trends Cell Biol 13: 79-85, 2003.
26. Jacinto E and Hall MN: Tor signalling in bugs, brain and brawn. Nat Rev Mol Cell Biol 4: 117-126, 2003.
27. Dancey JE: Clinical development of mammalian target of rapamycin inhibitors. Hematol Oncol Clin North Am 16: 1101-1114, 2002.
28. Huang S and Houghton PJ: Targeting mTOR signaling for cancer therapy. Curr Opin Pharmacol 3: 371-377, 2003.
29. Philp AJ, Campbell IG, Leet C, Vincan E, Rockman SP, Whitehead RH, Thomas RJ and Phillips WA: The phosphatidylinositol 3'-kinase p85alpha gene is an oncogene in human ovarian and colon tumors. Cancer Res 61: 7426-7429, 2001.
30. Fingar DC, Richardson CJ, Tee AR, Cheatham L, Tsou C and Blenis J: mTOR controls cell cycle progression through its cell growth effectors S6K1 and 4E-BP1/eukaryotic translation initiation factor 4E. Mol Cell Biol 24: 200-216, 2004.
31. Hardie DG: New roles for the LKB1→AMPK pathway. Curr Opin Cell Biol 17: 167-173, 2005.
32. Mantzoros C, Petridou E, Dessypris N, Chavelas C, Dalamaga M, Alexe DM, Papadiamantis Y, Markopoulos C, Spanos E, Chrousos G and Trichopoulos D: Adiponectin and breast cancer risk. J Clin Endocrinol Metab 89: 1102-1107, 2004.
33. Miyoshi Y, Funahashi T, Kihara S, Taguchi T, Tamaki Y, Matsuzawa Y and Noguchi S: Association of serum adiponectin levels with breast cancer risk. Clin Cancer Res 9: 5699-5704, 2003.
34. Petridou E, Mantzoros C, Dessypris N, Koukoulomatis P, Addy C, Voulgaris Z, Chrousos G and Trichopoulos D: A case-control study in Greece. J Clin Endocrinol Metab 88: 993-997, 2003.
35. Petridou E, Mantzoros C, Dessypris N, Koukoulomatis P, Addy C, Voulgaris Z, Chrousos G and Trichopoulos D: Circulating adiponectin and endometrial cancer risk. J Clin Endocrinol Metab 89: 1160-1163, 2004.
36. Otake S, Takeda H, Suzuki Y, Fukui T, Watanabe S, Ishihama K, Saito T, Togashi H, Nakamura T, Matsuzawa Y and Kawata S: Association of visceral fat accumulation and plasma adiponectin with colorectal adenoma: evidence for participation of insulin resistance. Clin Cancer Res 11: 3642-3646, 2005.
37. Yoneda K, Tomimoto A, Endo H, Iida H, Sugiyama M, Takahashi H, Mawatari H, Nozaki Y, Fujita K, Yoneda M, Inamori M, Nakajima N, Wada K, Nagashima Y, Nakagama H, Uozaki H, Fukayama M and Nakajima A: Expression of adiponectin receptors, AdipoR1 and AdipoR2, in normal colon epithelium and colon cancer tissue. Oncol Rep 20: 479-483, 2008.
38. Schmelzle T and Hall MN: TOR, a central controller of cell growth. Cell 103: 253-262, 2000.
39. Panwalkar A, Verstovsek S and Giles FJ: Mammalian target of rapamycin inhibition as therapy for hematologic malignancies. Cancer 101: 1478, 2004.
40. De Young MP, Horak P, Sofer A, Sgroi D and Ellisen LW: Hypoxia regulates TSC1/2-mTOR signaling and tumor suppression through REDD1-mediated 14-3-3 shuttling. Genes Dev 15: 239-251, 2008.
41. McCubrey JA, Steelman LS, Abrams SL, Bertrand FE, Ludwig DE, Bäsecke J, Libra M, Stivala F, Milella M, Tafuri A, Lunghi P, Bonati A and Martelli AM: Targeting survival cascades induced by activation of Ras/Raf/MEK/ERK, PI3K/PTEN/Akt/mTOR and Jak/STAT pathways for effective leukemia therapy. Leukemia 22: 708-722, 2008.

Association of visceral fat accumulation and plasma adiponectin with rectal dysplastic aberrant crypt foci in a clinical population

Hirokazu Takahashi,[1,5] Tetsuji Takayama,[2] KyokoYoneda,[1] Hiroki Endo,[1] Hiroshi Iida,[1] Michiko Sugiyama,[1] Koji Fujita,[1] Masato Yoneda,[1] Masahiko Inamori,[1] Yasunobu Abe,[1] Satoru Saito,[1] Koichiro Wada,[3] Hitoshi Nakagama[4] and Atsushi Nakajima[1]

[1]Gastroenterology Division, Yokohama City University Graduate School of Medicine, Yokohama, Kanagawa 236-0004; [2]Gastroenterology Division, University of Tokushima Faculty of Medicine, Tokushima 770-8503; [3]Department of Pharmacology, School of Dentistry, Osaka University, Osaka 565-0871; [4]Biochemistry Division, National Cancer Center Research Institute, Tokyo 104-0045, Japan

(Received June 21, 2008/Revised August 31, 2008/Accepted September 5, 2008/Online publication October 23, 2008)

The association between obesity and the risk of colorectal cancer (CRC) cannot be easily evaluated because CRC itself is associated with a gradual loss of bodyweight. Aberrant crypt foci (ACF) can be classified as dysplastic ACF or non-dysplastic ACF by magnifying colonoscopy, and dysplastic ACF are thought to be a biomarker of CRC. Ninety-four participants who underwent colonoscopy at Yokohama City University Hospital, Japan, were enrolled in the current study. We detected 557 ACF, including 67 dysplastic ACF (12.0%). Univariate regression analysis was conducted to determine correlations between the number of dysplastic ACF and various potential risk factors, including patient age, waist circumference, body mass index, visceral fat area (VFA), and plasma adiponectin level. The results of multiple regression analysis revealed that the number of dysplastic ACF correlated with age (correlation coefficient $r = 0.212$, $P = 0.0383$) and plasma adiponectin level ($r = -0.201$, $P = 0.0371$), even after adjustments for sex, waist circumference, body mass index, and VFA. Our univariate correlation analysis data showed a significant correlation with the number of dysplastic ACF with VFA ($r = 0.238$, $P = 0.0209$), no correlation with subcutaneous fat area, and an inverse correlation with the plasma level of adiponectin ($r = -0.258$, $P = 0.0118$). Thus, our results suggest that aging and visceral fat accumulation could correlate moderately with colorectal carcinogenesis. The novelty of our study lies in the finding that visceral fat accumulation and a low plasma adiponectin level may promote colorectal carcinogenesis; therefore, these obesity-related parameters may serve as novel targets for CRC prevention. (*Cancer Sci* 2009; 100: 29–32)

Obesity and its associated visceral fat accumulation have been reported to be linked to an elevated risk of cardiovascular disease, diabetes mellitus, and mortality, and these complications are rapidly becoming significant problems.[1,2] Visceral adipose tissue is not only fat storage tissue, but also a metabolically active organ secreting many adipocytokines, such as adiponectin.[3] Obesity is reportedly an important risk factor for CRC.[4] CRC has high mortality and morbidity rates, and its prevalence has been increasing.[5,6] The precise risk factors for CRC remain unclear, although a family history and several dietary and lifestyle factors have been proposed to be involved.[7]

The association between obesity and the risk of CRC cannot be easily evaluated because of the confounding effect of bodyweight loss with CRC. Therefore, we sought to identify a biomarker for risk assessment and monitoring of CRC. ACF, which were first discovered in mice treated with azoxymethane,[8] have been clearly shown to be precursor lesions of CRC, and are now established as a biomarker of the risk of CRC in azoxymethane-treated mice and rats.[9] In humans, ACF can be classified as dysplastic or non-dysplastic through the use of magnifying colonoscopy.[10] ACF have not been firmly established to be precursors of CRC; however, dysplastic ACF could possibly serve as a biomarker of the risk of CRC. Previous studies have reported that individuals with CRC have more ACF than those without CRC, therefore dysplastic ACF represent potential clinical precursors of CRC and colorectal adenoma.[11–14] Recently, an association was suggested to exist between obesity and the risk of CRC.[15,16] However, the relationship between obesity and ACF remains unclear. Therefore, the current study in a clinical population aimed to investigate the relationship between various obesity-associated parameters and rectal dysplastic ACF.

Patients and Methods

Study population. We prospectively evaluated 94 subjects recruited from the population of healthy individuals who underwent colonoscopy at Yokohama City University Hospital, Japan. The exclusion criteria included: presence of contraindications to colonoscopy; current or past non-steroidal anti-inflammatory drug use including aspirin; family history of CRC; or history of adenoma, carcinoma, familial adenomatous polyposis, inflammatory bowel disease, or radiation colitis. Subjects with a history of colectomy, gastrectomy, or colorectal polypectomy, and those treated with daily insulin self-injection or sulfonylurea for diabetes mellitus, were also excluded. In order to investigate the influence of obesity on colorectal carcinogenesis, patients with colorectal adenoma or carcinoma at the time of colonoscopy were also excluded from the study. Written informed consent was obtained from all subjects prior to their participation. The study protocol was approved by the Yokohama City University Hospital Ethics Committee.

Collection and analysis of blood samples for adiponectin level. Blood samples were obtained in the morning on the day of colonoscopy after overnight fasting. Plasma adiponectin levels were measured by enzyme-linked immunosorbent assay of the total forms of human adiponectin (SRL Co., Tokyo, Japan).

Magnifying colonoscopy for identification of ACF. Participants' bowel preparation for the colonoscopy was carried out using

[5]To whom correspondence should be addressed.
E-mail: hirokazu@med.yokohama-cu.ac.jp
Abbreviations: ACF, aberrant crypt foci; BMI, body mass index; CRC, colorectal cancer; CT, computed tomography; SFA, subcutaneous fat area; TFA, total fat area; VFA, visceral fat area.

doi: 10.1111/j.1349-7006.2008.00994.x

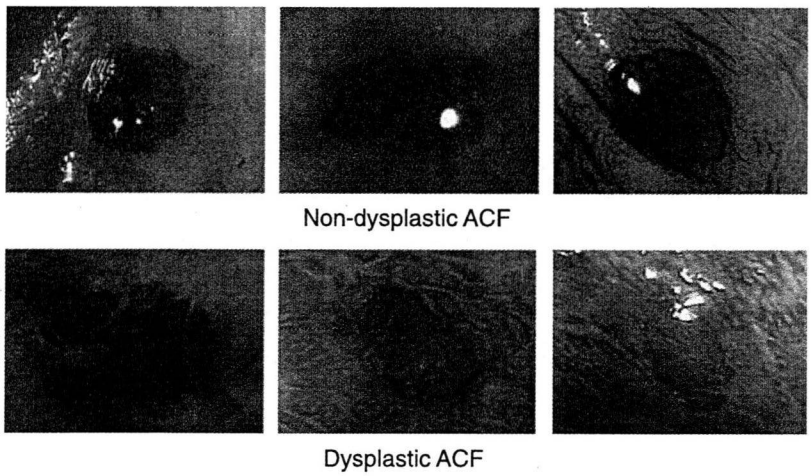

Fig. 1. Typical features of non-dysplastic and dysplastic aberrant crypt foci (ACF) on magnifying colonoscopy after methylene blue staining.

polyethylene glycol solution. A Fujinon EC-490ZW5/M colonoscope was used for the magnifying colonoscopy (Fujinon Toshiba ES Systems, Tokyo, Japan). Total colonoscopy was carried out before imaging of rectal ACF. Subsequently, 0.25% methylene blue was applied to the mucosa with a spray catheter. Aberrant crypts were distinguished from normal crypts by their deeper staining and larger diameter, and the number of ACF in the rectum was counted. This counting was conducted in the lower rectal region, extending from the middle Houston valve to the dentate line, based on the results of a previous study.[10] All ACF were recorded photographically and evaluated by two independent observers who were unaware of the subjects' clinical histories.

Criteria used for endoscopic diagnosis. ACF were defined as lesions in which the crypts were more darkly stained with methylene blue than normal crypts and had larger diameters, often with oval or slit-like lumens and a thicker epithelial lining.[17–20] Dysplastic ACF were defined as crypts in which each lumen was compressed or not distinct, with an epithelial lining that was much thicker than that of normal surrounding crypts. Non-dysplastic ACF were classified as hyperplastic or non-hyperplastic.[10]

Measurement of VFA and SFA. BMI was calculated using the following equation: bodyweight (kg)/(height [m]^2). Intra-abdominal adipose tissue was assessed, as described previously by measuring the VFA, SFA, TFA, and waist circumference from CT images at the level of the umbilicus.[4,10] All CT scans were carried out with the subjects in the supine position. The borders of the intra-abdominal cavity were outlined on the CT images, and the VFA was quantified using Fat Scan software (N2 System Corporation, Kobe, Japan).

Statistical analysis. We examined the associations between the risk factors for CRC and the number of dysplastic ACF. All data were expressed as mean ± SD, unless otherwise indicated. The relationships between the number of dysplastic ACF and relevant covariates were examined by univariate regression analysis, and standardized correlation coefficients were determined using Stat View software (SAS Institute, Cary, NC, USA). Multiple regression analysis was carried out to assess the relationship between the number of dysplastic ACF and potentially associated variables, and to determine the standardized correlation coefficients. The dependent variable was the number of dysplastic ACF, and the independent variables were age, sex, VFA, and plasma adiponectin level. Waist circumference and BMI were excluded from this analysis because these factors have a high correlation with VFA. P-values < 0.05 were considered to denote statistical significance.

Results

Colonoscopic features of ACF. A total of 557 ACF, including 67 dysplastic ACF, were counted by magnifying colonoscopy in the 94 patients. The aberrant crypts were larger, thicker, and more darkly stained than the normal crypts. Dysplastic ACF and non-dysplastic ACF accounted for 12.0% (67 of 557) and 88.0% (490 of 557) of the total, respectively. The number of subjects with dysplastic ACF was 34, and the number with non-dysplastic ACF was 76. In the lesions detected by magnifying colonoscopy, the size (i.e. median number of crypts ± SD) per ACF was 15.1 ± 10.4 and per dysplastic ACF was 8.5 ± 11.8. The average number of composition crypts per ACF was 93.2 ± 124.3 and per dysplastic ACF was 16.3 ± 26.2. In the 94 patients, the mean total number of ACF (non-dysplastic and dysplastic) per patient was 5.92 ± 6.50, and the mean number of dysplastic ACF per patient was 0.71 ± 1.16. The typical colonoscopic features of dysplastic and non-dysplastic ACF are shown in Figure 1.

Patient characteristics. The clinical characteristics of the study participants are shown in Table 1. The mean age was 65.1 ± 10.8 years, and there were 48 men and 46 women. The mean waist circumference, BMI, TFA, VFA, SFA, and plasma adiponectin level were 86.3 ± 10.0 cm, 23.3 ± 3.1 kg/m^2, 200.8 ± 91.4 cm^2, 83.9 ± 50.1 cm^2, 116.7 ± 60.4 cm^2, and 11.0 ± 5.6 μg/mL, respectively.

Univariate regression analysis: Correlations between risk factors for CRC and the number of dysplastic ACF. Age correlated significantly with the number of dysplastic ACF, as shown in Table 2 ($r = 0.232$, $P = 0.0242$). Sex showed no correlation with the number of dysplastic ACF. All of the obesity parameters, except SFA ($r = -0.001$, $P = 0.9979$), correlated significantly with the number of dysplastic ACF,* as follows: waist circumference ($r = 0.225$, $P = 0.0293$), BMI ($r = 0.307$, $P = 0.0325$), and VFA ($r = 0.238$, $P = 0.0209$). The plasma level of adiponectin showed a significant inverse correlation with the number of dysplastic ACF ($r = -0.258$, $P = 0.0118$). Age was the only parameter that correlated significantly with the number of non-dysplastic ACF ($r = 0.218$, $P = 0.0336$), which were much more abundant than dysplastic ACF in the study subjects.

Multiple regression analysis: Correlations between risk factors for CRC and the number of dysplastic ACF. The results of the multiple regression analysis are shown in Table 3. After adjustments for sex, waist circumference, BMI, and VFA, the parameters of age and plasma adiponectin level still correlated significantly with the number of dysplastic ACF ($P = 0.0383$ and $P = 0.0371$, respectively).

doi: 10.1111/j.1349-7006.2008.00994.x

Table 1. Clinical characteristics of study participants

Characteristic	Overall	Subjects with non-dysplastic ACF	Subjects with dysplastic ACF
Number	94	76	34
Age (years)	65.1 ± 10.8	66.3 ± 10.1	66.2 ± 8.1
Sex (male : female)	48:46	43:33	21:13
Waist circumference (cm)	86.3 ± 10.0	86.0 ± 10.5	88.4 ± 11.2
Body mass index (kg/m^2)	23.3 ± 3.1	23.3 ± 3.2	24.2 ± 3.0
Total fat area (cm^2)	200.8 ± 91.4	199.5 ± 95.7	222.0 ± 96.0
Visceral fat area (cm^2)	83.9 ± 50.1	86.3 ± 51.6	103.6 ± 52.6
Ssubcutaneous fat area (cm^2)	116.7 ± 60.4	112.9 ± 60.8	117.8 ± 58.4
Plasma adiponectin (μg/mL)	11.0 ± 5.6	11.3 ± 5.8	9.4 ± 4.3

Data are expressed as mean ± SD. ACF, aberrant crypt foci.

Table 2. Univariate correlation analysis: Correlations between the number of non-dysplastic or dysplastic aberrant crypt foci (ACF) and the risk factors for colorectal cancer

Risk factor	Non-dysplastic ACF		Dysplastic ACF	
	r	*P*	*r*	*P*
Age	0.218	0.0336*	0.232	0.0242*
Sex	0.109	0.2928	0.087	0.4069
Waist circumference	0.076	0.4651	0.225	0.0293*
Body mass index	0.169	0.1011	0.307	0.0325*
Total fat area	0.126	0.2257	0.135	0.1941
Visceral fat area	0.137	0.1868	0.238	0.0209*
Subcutaneous fat area	0.078	0.4560	−0.001	0.9979
Plasma adiponectin	−0.019	0.8538	−0.258	0.0118*

Age, waist circumference, body mass index, visceral fat area, and plasma adiponectin level correlated with the number of dysplastic ACF.
*$P < 0.05$.

Table 3. Multiple regression analysis: Correlations between the number of dysplastic aberrant crypt foci and the risk factors for colorectal cancer

Risk factor	Correlation coefficient	*P*
Age	0.212	0.0383*
Sex	0.038	0.7141
Waist circumference	−0.152	0.4508
Body mass index	0.249	0.1618
Visceral fat area	0.089	0.5807
Plasma adiponectin	−0.201	0.0371*

R^2 for the entire model = 0.368.
After adjustments for sex, waist circumference, body mass index, and visceral fat area, the parameters of age and plasma adiponectin level still correlated with the number of dysplastic aberrant crypt foci.
*$P < 0.05$.

Discussion

In the present study a total of 557 ACF were counted in the 94 patients, and we demonstrated a significant correlation between the number of dysplastic ACF and the VFA, and a significant inverse correlation between the number of dysplastic ACF and the plasma adiponectin level. Age was also associated with the number of ACF, that is, the number of dysplastic and non-dysplastic ACF increased with age. CRC is thought to progress through several morphological stages, from the formation of polyps to the onset of malignant change.[21] Genetic alterations, including mutations in the *K-ras*, *p53*, and *APC* genes, have been reported to be associated with the disease progression.[22] The *K-ras* mutation has also been reported in human ACF.[23] Therefore, the increased risk of ACF formation with age may be influenced mainly by these genetic alterations. Sex showed no correlation with the number of dysplastic ACF in the present study; however, the incidence of CRC is lower in women than in men.[24,25] It has been suggested that the initiation of dysplastic ACF is comparable in men and women, but thereafter tumor progression differs because visceral fat accumulation is higher in men than woman. This visceral fat accumulation may affect tumor progression.

Waist circumference has often been suggested to be associated with VFA. Consistent with this suggestion, our data showed that both waist circumference and VFA were associated with the number of dysplastic ACF. Recent reports have suggested that obesity may be associated with a high risk of CRC.[4] Several studies have shown that increased BMI is associated with an increased risk of CRC.[26] The importance of the size of ACF has been reported,[27] and the correlation between size, measured as the median number of crypts per both non-dysplastic ACF and dysplastic ACF, and risk factors was analyzed. The correlation between the median number of crypts per ACF and any risk factors had almost the same result as the number of ACF (data not shown). Our data showed a direct correlation between the VFA and the number of dysplastic ACF, and an inverse correlation between the plasma adiponectin level and the number of dysplastic ACF (Table 2). A previous study showed that the *K-ras* gene was mutated in 50–60% of patients with dysplastic ACF,[10] thus genetic alterations were already underway. Visceral fat correlated with dysplastic ACF in the current study, and another study showed that increased visceral adiposity was a significant predictor of lower rates of disease-free survival in patients with resectable colorectal cancer,[28] suggesting that visceral fat plays an important role in colorectal carcinogenesis and progression. Visceral fat tissue is known to be an endocrine organ that secretes adiponectin, which has an inverse relationship with obesity and visceral fat.[29] We carried out multiple regression analysis to assess whether plasma adiponectin may be a risk factor for dysplastic ACF growth, independent of the effects of obesity. If dysplastic ACF are a biomarker of the risk of colorectal adenoma and CRC, then some factors associated with the risk of CRC may also influence the number of dysplastic ACF. Very little is known about the factors that initiate or promote the growth of dysplastic ACF in humans. Our results suggest that plasma adiponectin levels are inversely associated with the number of ACF, and that visceral fat may be associated directly with ACF and thus could be a risk factor for the early stage of colorectal carcinogenesis.

There are many reports on the existence of relationships between the risk of CRC and exercise, energy use, glycemic index, and food choices and dietary constituents.[30–32] These factors affect each other, therefore it is difficult to evaluate the relationship between any one factor and the risk of CRC. Obesity

is thought to result from many of these factors. It is also thought that aging, visceral fat, and adiponectin are important in CRC carcinogenesis. Further investigation is needed to elucidate the mechanisms that affect these relationships and the impact on the development of CRC.

The novelty of our study lies in our use of dysplastic ACF as a biomarker for risk of CRC to show that visceral fat accumulation and low plasma adiponectin level may affect colorectal carcinogenesis. Further studies should be conducted to clarify the role that visceral fat accumulation and reduced plasma adiponectin play in dysplastic ACF growth and whether these obesity-related parameters may serve as novel targets for CRC prevention.

Acknowledgments

We thank Machiko Hiraga for her technical assistance. This work was supported in part by a Grant-in-Aid for research on the Third Term Comprehensive Control Research for Cancer from the Ministry of Health, Labour, and Welfare, Japan to A.N., a grant from the National Institute of Biomedical Innovation to A.N., a grant from the Ministry of Education, Culture, Sports, Science, and Technology, Japan (KIBAN-B) to A.N., a grant from the Ministry of Education, Culture, Sports, Science, and Technology, Japan (WAKATE-B) to H.T., a research grant from the Princess Takamatsu Cancer Research Fund to A.N., and a grant for the 2007 Strategic Research Project (no. K19041) of Yokohama City University, Japan to H.T. and A.N.

References

1 Fujioka S, Matsuzawa Y, Tokunaga K *et al.* Contribution of intra-abdominal fat accumulation to the impairment of glucose and lipid metabolism in human obesity. *Metabolism* 1987; **36**: 54–9.
2 Kissebah AH, Vydelingum N, Murray R *et al.* Relation of body fat distribution to metabolic complications of obesity. *J Clin Endocrinol Metab* 1982; **54**: 254–60.
3 Park KG, Park KS, Kim MJ *et al.* Relationship between serum adiponectin and leptin concentrations and body fat distribution. *Diabetes Res Clin Pract* 2004; **63**: 135–42.
4 Giovannucci E, Aasherio A, Rimm EB *et al.* Physical activity, obesity, and risk for colon cancer and adenoma in men. *Ann Intern Med* 1995; **122**: 327–34.
5 Anderson WF, Umar A, Brawley OW. Colorectal carcinoma in black and white race. *Cancer Metastasis Rev* 2003; **22**: 67–82.
6 Rougier P, Mitry E. Epidemiology, treatment and chemoprevention in colorectal cancer. *Ann Oncol* 2003: **14**: ii3–5.
7 Garland C, Shekelle RB, Barrett-Connor E *et al.* Dietary vitamin D and calcium and risk of colorectal cancer: a 19-year prospective study in men. *Lancet* 1985; **1**: 307–9.
8 Bird RP. Observation and quantification of aberrant crypts in the murine colon treated with a colon carcinogen: preliminary findings. *Cancer Lett* 1987; **37**: 147–51.
9 Pretlow TP, O'Riordan MA, Somich GA *et al.* Aberrant crypts correlate with tumor incidence in F344 rats treated with azoxymethane and phytate. *Carcinogenesis* 1992; **13**: 1509–12.
10 Takayama T, Katsuki S, Takahashi Y *et al.* Aberrant crypt foci of the colon as precursors of adenoma and cancer. *N Engl J Med* 1998; **339**: 1277–84.
11 Nascimbeni R, Villanacci V, Mariani PP *et al.* Aberrant crypt foci in the human colon: frequency and histologic patterns in patients with colorectal cancer or diverticular disease. *Am J Surg Pathol* 1999; **23**: 1256–63.
12 Shpitz B, Bomstein Y, Mekori Y *et al.* Aberrant crypt foci in human colons: distribution and histomorphologic characteristics. *Hum Pathol* 1998; **29**: 469–75.
13 Adler DG, Gostout CJ, Sorbi D *et al.* Endoscopic identification and quantification of aberrant crypt foci in the human colon. *Gastrointest Endosc* 2002; **56**: 657–62.
14 Nucci MR, Robinson CR, Longo P *et al.* Phenotypic and genotypic characteristics of aberrant crypt foci in human colorectal mucosa. *Hum Pathol* 1997; **28**: 1396–407.
15 Gunter MJ, Leitzmann MF. Obesity and colorectal cancer: epidemiology, mechanisms and candidate genes. *J Nutr Biochem* 2006; **17**: 145–56.
16 Otake S, Takeda H, Suzuki Y *et al.* Association of visceral fat accumulation and plasma adiponectin with colorectal adenoma: evidence for participation of insulin resistance. *Clin Cancer Res* 2005; **11**: 3642–6.
17 Roncucci L, Stamp D, Medline A *et al.* Identification and quantification of aberrant crypt foci and microadenomas in the human colon. *Hum Pathol* 1991; **22**: 287–94.
18 Roncucci L, Medline A, Bruce WR. Classification of aberrant crypt foci and microadenomas in human colon. *Cancer Epidemiol Biomarkers Prev* 1991; **1**: 57–60.
19 Pretlow TP, Barrow BJ, Ashton WS *et al.* Aberrant crypts: putative preneoplastic foci in human colonic mucosa. *Cancer Res* 1991; **51**: 1564–7.
20 Pretlow TP, O'Riordan MA, Pretlow TG *et al.* Aberrant crypts in human colonic mucosa: putative preneoplastic lesions. *J Cell Biochem Suppl* 1992; **16**: 55–62.
21 Kinzler KW, Vogelstein B. Lessons from hereditary colorectal cancer. *Cell* 1996; **87**: 159–70.
22 Fearon ER, Vogelstein B. A genetic model for colorectal tumorigenesis. *Cell* 1990; **61**: 759–67.
23 Yuan P, Sun MH, Zhang JS *et al.* APC and K-ras gene mutation in aberrant crypt foci of human colon. *World J Gastroenterol* 2001; **7**: 352–6.
24 Gao RN, Neutel CI, Wai E. Gender differences in colorectal cancer incidence, mortality, hospitalizations and surgical procedures in Canada. *J Public Health* 2008; **30**: 194–201.
25 de Kok IM, Wong CS, Chia KS *et al.* Gender differences in the trend of colorectal cancer incidence in Singapore, 1968–2002. *Int J Colorectal Dis* 2008; **23**: 461–7.
26 Graham S, Marshall J, Haughey B *et al.* Dietary epidemiology of cancer of the colon in western New York. *Am J Epidemiol* 1988; **128**: 490–503.
27 Rudolph RE, Dominitz JA, Lampe JW *et al.* Risk factors for colorectal cancer in relation to number and size of aberrant crypt foci in humans. *Cancer Epidemiol Biomarkers Prev* 2005; **14**: 605–8.
28 Moon HG, Ju YT, Jeong CY *et al.* Visceral obesity may affect oncologic outcome in patients with colorectal cancer. *Ann Surg Oncol* 2008; **15**: 1918–22.
29 Arita Y, Kihara S, Ouchi N *et al.* Paradoxical decrease of an adipose-specific protein, adiponectin, in obesity. *Biochem Biophys Res Commun* 1999; **257**: 79–83.
30 Gerhardsson M, Floderus B, Norell SE. Physical activity and colon cancer risk. *Int J Epidemiol* 1988; **17**: 743–6.
31 Slattery ML, Benson J, Berry TD *et al.* Dietary sugar and colon cancer. *Cancer Epidemiol Biomarkers Prev* 1997; **6**: 677–85.
32 Reedy J, Haines PS, Steckler A *et al.* Qualitative comparison of dietary choices and dietary supplement use among older adults with and without a history of colorectal cancer. *J Nutr Educ Behav* 2005; **37**: 252–8.

doi: 10.1111/j.1349-7006.2008.00994.x

Genes and Environment, Vol. 31, No. 1 pp. 9-14 (2009)

Regular article

Mutagenic Specificity of *N*-Nitrosotaurocholic Acid in *supF* Shuttle Vector Plasmids

Masanobu Kawanishi[1], Hiroshi Nishida[1], Yukari Totsuka[2], Koichi Nishimura[2], Keiji Wakabayashi[2] and Takashi Yagi[1,3]

[1]Environmental Genetics Laboratory, Frontier Science Innovation Center and Graduate School of Science, Osaka Prefecture University, Osaka, Japan
[2]Cancer Prevention Basic Research Project, National Cancer Center Research Institute, Tokyo, Japan

(Received June 30, 2008; Revised August 11, 2008; Accepted August 20, 2008)

The mutagenic specificity of *N*-nitrosotaurocholic acid (NO-TCA) in human cells was investigated using *supF* shuttle vector plasmids. The plasmids pMY189 were treated with NO-TCA *in vitro* and introduced into normal fibroblasts (WI38-VA13) and nucleotide excision repair (NER)-deficient cells (XP2OS(SV)) for replication. The background mutation frequency of the *supF* gene was 4.1×10^{-4} and 2.0×10^{-4} after replication in normal and NER-deficient cells, respectively. The mutation frequency increased 5 and 15 times in normal and NER-deficient cells, respectively, after the treatment of the plasmid with 50 mg/mL of NO-TCA. The higher mutation frequency in NER-deficient cells indicates that the DNA damage induced by NO-TCA is repaired by NER. Base sequence analysis of 101 and 94 plasmids with mutations in the *supF* gene propagated in normal and NER-deficient cells, respectively, revealed that the majority of the mutations were base substitutions (about 89 and 90%) and the rest were deletions and insertions (about 11 and 10%) in both cell lines. About half of the mutant plasmids contained a single base substitution. Of the single base substitutions, the most frequent mutations were G:C to A:T transitions (about 37 and 36%), followed by G:C to C:G transversions (about 31 and 28%) in both cell lines. The mutations were not distributed randomly but were located at several hot spots in the *supF* gene, and almost all hot spots were at G:C sites. These observations accord with previous findings that NO-TCA forms DNA adducts with dC and induces G:C to A:T base substitution in *Salmonella typhimurium* TA100.

Key words: *N*-nitrosotaurocholic acid, mutagenic specificity, *supF* shuttle vector plasmid

Introduction

Bile acids are components of bile, which is a digestive secretion produced in the mammalian liver and stored in the gallbladder. Bile acids are conjugated with glycine or taurine after their synthesis in hepatocytes. The conjugates are then excreted into the digestive tract. Bile acids have been treated as carcinogens for more than half a century, and recent reports indicate that bile acids cause DNA damage (1). Epidemiological studies indicate an association between bile acids and colorectal cancer (2,3), and high levels of secondary bile acids are present in the feces of populations at high risk of colorectal cancer (4,5).

Nitrosation of bile acid conjugates can be mediated by the acid-catalyzed reaction of amides with nitrite (6), and activated macrophages in infected and inflamed organs are also believed to be involved in such reactions. *N*-Nitroso bile acid conjugates have been suggested as plausible etiological factors in the development of gastric cancer in humans (7,8). *N*-Nitrosotaurocholic acid (NO-TCA), an *N*-nitroso bile acid conjugate, has already been demonstrated to exert mutagenic activity in both bacterial and mammalian assay systems (6,9). NO-TCA induces hepatocellular carcinoma and gastric tumors in male Fischer 344 rats (10). Recently, the chemical structures of DNA adducts derived from NO-TCA were identified. NO-TCA reacts directly with DNA and forms the DNA adduct, 3-ethanesulfonic acid-2′-deoxycytidine (3-ethanesulfonic acid-dC), N^4-cholyl-2′-deoxycytidine (N^4-cholyl-dC), and N^6-cholyl-2′-deoxyadenosine (N^6-cholyl-dA) (11). In a ^{32}P-postlabeling assay, adduct spots corresponding to 3-ethanesulfonic acid-dC were detected in both duodenal reflux and sham operation rats (12). NO-TCA induced mutations in *Salmonella typhimurium* TA100, and a mutation spectrum analysis revealed that NO-TCA predominantly induced G:C to A:T transitions (11). However, the mutation spectrum of NO-TCA in mammalian cells has not been investigated.

Shuttle vector plasmids are used to examine the spec-

[3]Correspondence to: Takashi Yagi, Environmental Genetics Laboratory, Frontier Science Innovation Center, Osaka Prefecture University, 1-2 Gakuen-cho, Naka-ku, Sakai, Osaka 599-8570, Japan. Tel: +81-72-254-9862, Fax: +81-72-254-9938, E-mail: yagi-t@riast.osakafu-u.ac.jp

trum of mutations caused by environmental mutagens and carcinogens (13). The mutations induced in the plasmids by mutagens reflect the mutations that occur in endogenous genes of mammalian cells in which the plasmids are propagated (14). In the present study, we used the pMY189 plasmid (15), a derivative of the pZ189 shuttle vector plasmids, to analyze mutational specificity. The plasmids were treated with NO-TCA, and the frequencies and types of NO-TCA-induced mutations in the *supF* gene of plasmids in normal and repair deficient human cells were analyzed.

Materials and Methods

Chemicals: NO-TCA was purchased from the Nard Institute (Osaka, Japan). Ampicillin, chloramphenicol, nalidixic acid, isopropyl β-D-thiogalactoside (IPTG), and 5-bromo-4-chloro-3-indoyl β-D-galactoside (X-gal) were obtained from Sigma-Aldrich Japan (Tokyo, Japan). Restriction endonuclease *Dpn*I was purchased from New England Biolabs (Beverly, MA, USA).

Cells: SV40-transformed normal human fibroblast cells, WI38-VA13 (16), and group A nucleotide excision repair (NER)-deficient cells XP2OS(SV) were used (17). All cells were cultured in RPMI1640 medium (Sigma-Aldrich Japan) supplemented with 10% fetal bovine serum (JRH Biosciences, Lenexa, KS, USA).

Shuttle vector plasmid and bacterial strains: The shuttle vector plasmid pMY189, which is a derivative of the pZ189 plasmid (13), was used for the mutation analysis (15). The indicator *E. coli* strain KS40/pKY241 (18) is a nalidixic acid-resistant (*gyrA*) derivative of MBM7070 [*lacZ* (am) *CA7070 lacY1 HsdR HsdM D* (*araABC-leu*)*7679 galU galK rpsL thi*] (19), and was used to detect the mutated *supF* of pMY189. The plasmid pKY241 was constructed by Akasaka *et al.* (18) and contains a chloramphenicol resistant marker and *gyrA* (amber) genes. *E. coli* KS40/pKY241 cells that carry the active *supF* gene cannot form colonies on a plate containing nalidixic acid, whereas the cells that carry the mutated *supF* gene can form colonies on selection plates containing nalidixic acid, chloramphenicol, and ampicillin. *E. coli* cells containing the wild type *supF* gene produce blue colonies, whereas cells containing the mutated *supF* gene produce white or light blue colonies on the selection plates.

Treatment of the plasmid with NO-TCA, transfection into human cells, and plasmid recovery: Purified stocks of pMY189 were prepared by using the QIAGEN plasmid purification kit (QIAGEN GmbH, Hilden, Germany). pMY189 (3 μg) was incubated with various amounts of NO-TCA in 33 μL of 100 mM phosphate buffer (pH 7.5) (11). The reaction was allowed to proceed for 6 h at 37°C followed by phenol/chloroform extraction and ethanol precipitation, and the plasmids were redissolved in 500 μL of Dulbecco's phosphate buffered saline (PBS) solution (pH 7.5). The WI38-VA13 or XP2OS(SV) (1×10^7 cells) cells and 3 μg of NO-TCA-treated pMY189 in PBS solution (500 μL) were placed in an electroporation cuvette (electrodes 0.4 cm apart), and the cells were transfected with the plasmids by an exponential electric pulse (350 V, 950 μF) using a Gene pulser Xcell (Bio-Rad Laboratories, Hercules, CA, USA). Transfection efficiency of the plasmids was almost same in both cell lines because the rate of plasmid recovery was not different in both cell lines using non-treated plasmid. The cells were plated in φ10 cm dishes and incubated at 37°C for 72 h in a CO_2 incubator. Then, the plasmids were extracted from the cultured cells using the QIAprep-spin miniprep kit (QIAGEN GmbH). The purified plasmids were digested with the restriction endonuclease *Dpn*I to eliminate plasmids that retained the bacterial methylation pattern.

Selection of mutated *supF* and determination of DNA base sequences: The *Dpn*I-treated plasmid DNA was introduced into the indicator bacteria KS40/pKY241 by the Micro Pulsar electroporation apparatus (Bio-Rad Laboratories). The bacterial cells were plated on Luria-Bertani (LB) agar containing 50 μg/mL nalidixic acid, 150 μg/mL ampicillin and 30 μg/mL chloramphenicol, IPTG, and X-gal to select the plasmids containing the mutated *supF* genes. A portion of the cells was plated on LB agar containing ampicillin and chloramphenicol to measure the total number of transformants. After the plates had been incubated for 24 h at 37°C, the colonies were counted, and mutation frequencies were calculated. After the *E. coli* that carried the mutated plasmids had been cultured overnight in 2 mL of LB medium, the plasmids were extracted and purified with the QIAprep-spin miniprep kit (QIAGEN GmbH), and the size of the mutated plasmid was checked by agarose gel electrophoresis. In order to reduce the contribution of spontaneous mutations, we selected *supF* mutants from plasmids treated with NO-TCA at the highest concentration. The base sequences of the *supF* gene of the plasmids that were not aberrant in size were determined with the ABI PRISM BigDye Terminator Cycle Sequencing Ready Reaction Kit v1.1 (Applied Biosystems Inc., Foster City, CA, USA) and the M13-21 primer using an ABI3130 automatic DNA sequencer (Applied Biosystems Inc.). Mutants that had identical base changes derived from the same transfection plate were not scored to exclude clusters of the same clones. The χ^2-goodness of fit test was used to determine if the NO-TCA-induced base substitution mutations were distributed randomly or non-randomly over the coding region of the *supF* tRNA gene.

Results

Mutation of plasmids: The mutation frequency increased in both cell lines with increasing concentrations

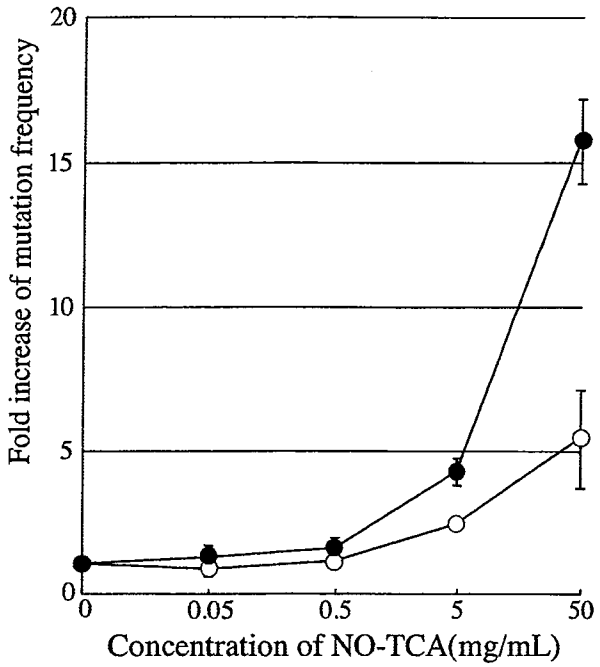

Fig. 1. The mutation frequency of the NO-TCA-treated pMY189 plasmids propagated in repair proficient WI38-VA13 (open circle) and repair deficient XP2OS(SV) cells (closed circle). The proportion of bacterial colonies containing the mutated *supF* gene in the ampicillin-resistant bacterial colonies is shown as the mutation frequency. The Y-axis represents the fold increase in the frequency when the background frequency is 1 (see text). The mean values of three independent experiments are plotted with the SD.

of NO-TCA (Fig. 1). The background plasmid mutation frequency was $2.0\text{–}4.1 \times 10^{-4}$ for both cell lines, and the mutation frequency increased about 5 and 15 times in the normal and XP cells, respectively, after treatment of the plasmid with 50 mg/mL of NO-TCA. The rate of plasmid recovery from the cells was not decreased by the NO-TCA treatment (data not shown).

Base sequence analysis: The majority (about 90 %) of the NO-TCA-induced mutations were base substitutions in both cell lines (Table 1). In XP cells, about 62 % and 25% of the mutant plasmids had single and multiple (at least two base substitutions except for tandem substitutions) base substitutions, respectively, and about 4% of them had tandem base substitutions (adjacent two base substitutions). In normal cells, about 51 and 36% of the plasmids had single and multiple base substitutions, respectively, and 3% of the plasmids had tandem base substitutions.

The types of single base substitutions found are shown in Table 2. The majority of the single base substitutions occurred at guanine or cytosine bases in both cell lines (about 94% and 86% in normal and XP cells, respectively). The most frequent mutations were G:C to A:T transitions, and the next most frequent mutations were G:C to C:G transversions in both cell lines.

Table 1. Types of sequence alterations in the *supF* gene in NO-TCA-treated plasmids pMY189 replicated in normal [WI38-VA13] or NER deficient [XP2OS(SV)] human fibroblasts

Type	No. of plasmids with mutations (%)	
	WI38-VA13	XP2OS(SV)
Base substitutions	90 (89.1)	85 (90.4)
Single	51 (50.5)	58 (61.7)
Multiple	36 (35.6)	23 (24.5)
Tandem	3 (3.0)	4 (4.2)
Frameshift	11 (10.9)	9 (9.6)
Deletion	10 (9.9)	8 (8.5)
Insertion	1 (1.0)	1 (1.1)
Total no. of plasmids sequenced	101 (100)	94 (100)

Table 2. Types of single base substitutions in the *supF* gene in NO-TCA-treated plasmids replicated in normal [WI38-VA13] or NER deficient [XP2OS(SV)] human fibroblasts

Base substitution	No. of base substitutions (%)	
	WI38-VA13	XP2OS(SV)
G:C to A:T	19 (37.2)	21 (36.2)
G:C to C:G	16 (31.4)	16 (27.6)
G:C to T:A	13 (25.5)	13 (22.4)
A:T to G:C	1 (2.0)	4 (7.0)
A:T to T:A	0 (0)	2 (3.4)
A:T to C:G	2 (3.9)	2 (3.4)
Total	51 (100)	58 (100)

Mutation spectrum: The locations of the NO-TCA-induced base substitutions in the coding region of the *supF* tRNA gene are shown in Fig. 2. The distribution was similar in normal and XP cells. Mutations were not distributed randomly ($p < 0.0001$ in both cells lines) but were mostly located at specific sites. There were several hot spots (at least three base changes occurred) at sites 133, 156, 159, 160, and 168 in normal cells and at sites 133, 156, 159, 160, 161, and 168 in XP cells, in which the number of the mutations observed was $\geq$4-fold greater than the number expected for a random distribution. The most prominent hot spot was at site 160 in both cells. All hot spots, except for site 161 in XP cells, were located at G:C sites.

Discussion

In the previous study, we reported that NO-TCA reacts with calf thymus DNA and forms 3-ethanesulfonic acid-dC and two bulky adducts: N^4-cholyl-dC and N^6-cholyl-dA (11). In the present study, the shuttle vector plasmds were treated with NO-TCA and introduced into normal and NER deficient cells. NER is known to be a major pathway by which cells remove bulky DNA

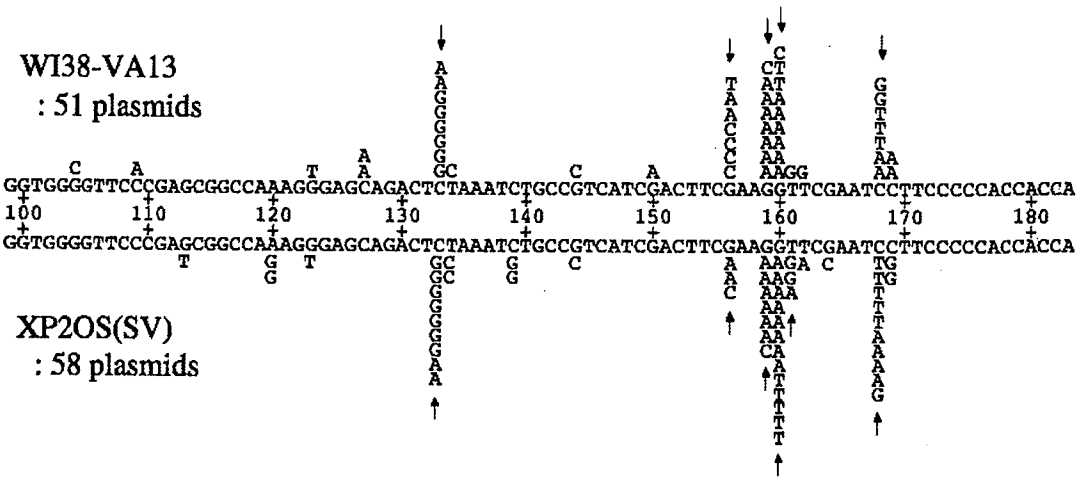

Fig. 2. The distribution of the NO-TCA-induced single base substitutions in the *supF* tRNA gene. Sites corresponding to tRNA coding sequences (residues 99–183) are shown. Substituted bases after plasmid replication in WI38-VA13 and XP2OS(SV) cells are shown above and below the tRNA coding sequence, respectively. The arrows indicate the locations of mutation hotspots.

adducts that had been induced by UV light and chemicals. As shown in Fig. 1, the mutation frequency was higher in the NER deficient XP cells than in the normal WI38 cells. Similar results have been reported with UV (13), *cis*-diamminedichloroplatinum (II) (20), and aflatoxin B1 (21), DNA lesions of which are known to be repaired by the NER system. These results suggest that the enhanced mutation frequencies induced by NO-TCA are due to unrepaired DNA adducts in cells and that NO-TCA adducts are removed from DNA by the NER system.

In an *S. typhimurium* assay, NO-TCA induced mutations in a dose-dependent manner in the TA100 strain, which can detect base substitution mutations, but did not induce mutations in the TA98 strain, which can detect frameshift mutations (11). In the present experiment, the majority (~90%) of the mutations induced in human cells were base substitutions, and frameshift mutations were rare (Table 1). The NO-TCA-produced DNA lesions caused base substitution mutations in both bacterial and mammalian cells. As shown in Table 1, about 25–36% of the NO-TCA-induced mutations were multiple base substitutions. There have been several reports on multiple substitutions in shuttle vector plasmids propagated in mammalian cells (22,23). Seidman *et al.* (22) explained that multiple substitutions are induced at undamaged bases by error-prone DNA polymerases. Courtemanche *et al.* (23) suggested that multiple mutations may arise during translesion DNA synthesis and involve an error-prone polymerase, which would introduce base opposite misinstructive or noninstructive base lesions and cause subsequent misincorporation errors. In the present study, to reveal the specific mutations induced by NO-TCA, we focused on single base substitutions since multiple base substitutions can contain base changes due to untargeted mutagenesis. As shown in Table 2, the most frequent single base substitution mutations were G:C to A:T transitions. This observation is consistent with the type of NO-TCA-induced mutations observed at the *hisG46* site of TA100 (11). Since this bacterial assay strain detects only reverse mutations, the information about base changes is limited. In contrast, the *supF* system can detect various types of mutation. In fact, the present study showed that about 31% and 26% of the single base substitutions were G:C to C:G and G:C to T:A transversions, respectively, in normal cells, while about 28% and 22% of them were G:C to C:G and G:C to T:A transversions, respectively, in XP cells (Table 2). We detected 3-ethanesulfonic acid-dC as a major adduct, and N^4-cholyl-dC and N^6-cholyl-dA as minor adducts in the reaction of NO-TCA with calf thymus DNA (11). We reported that the minor adduct signals were almost 500 times weaker than the major adduct signal in ^{32}P-postlabeling analysis (11). In the present work, most single base substitutions (about 94% and 86% in normal and XP cells, respectively) occurred at G:C sites and a small number of base substitutions (about 6% and 14% in normal and XP cells, respectively) were observed at A:T sites in the *supF* gene (Table 2). This base preference of mutations may reflect the relative amounts of dC and dA adducts in the plasmid.

As shown in Fig. 2, the single base substitutions occurred preferentially at certain sites. In the bacterial assay, NO-TCA induced G:C to A:T transitions at the CCC (*hisG46* site) of TA100. The *supF* gene contains several CCC (or GGG) sequences; however, none of the mutation hotspots were located at those sites in the present analysis. The CCC (or GGG) sequence might not be a hotspot of adduct formation. In fact, even if

NO-TCA induces base changes at other sequences, TA100 cannot detect them because its only mutation target site is *hisG46*. Other possibilities for the inconsistency of the mutation hotspots between these studies include differences in the damage-processing systems of *Salmonella* and human cells and differences in the method of NO-TCA treatment in these studies.

Specific mutations have been shown to be critical for the activation of oncogenes and the inactivation of tumor suppressor genes in human cancers. This work is the first report to describe the mutagenic specificity of NO-TCA in human cells. However, this study does not address the effect of chromatin structure, which may substantially affect adduct formation and mutagenesis. A comparison of NO-TCA-induced mutations in plasmid and chromosomal DNA is required for evaluation of its genetic effects in humans.

Acknowledgment: This work was supported by a Special Research Grant from Osaka Prefecture University, 2007, and by Grants-in-Aid from the Ministry of Education, Culture, Sports, Science and Technology and from the Ministry of Health, Labour and Welfare of Japan.

References

1 Bernstein H, Bernstein C, Payne CM, Dvorakova K, Garewal H. Bile acids as carcinogens in human gastrointestinal cancers. Mutat Res. 2005; 589: 47–65.

2 Debruyne PR, Bruyneel EA, Li X, Zimber A, Gespach C, Mareel MM. The role of bile acids in carcinogenesis. Mutat Res. 2001; 480–481: 359–69.

3 de Kok TM, van Maanen JM. Evaluation of fecal mutagenicity and colorectal cancer risk. Mutat Res. 2000; 463: 53–101.

4 Owen RW. Faecal steroids and colorectal carcinogenesis. Scand J Gastroenterol. 1997; 222 (Suppl): 76–82.

5 Kishida T, Taguchi F, Feng L, Tatsuguchi A, Sato J, Fujimori S, Tachikawa H, Tamagawa T, Yoshida Y, Kobayashi M. Analysis of bile acids in colon residual liquid or fecal material in patients with colorectal neoplasia and control subjects. J Gastroenterol. 1997; 32: 306–11.

6 Shuker DEG, Tannenbaum SR, Wishnok, JS. *N*-Nitroso bile acid conjugates. 1. Synthesis, chemical reactivity, and mutagenic activity. J Org Chem. 1981; 46: 2092–6.

7 Mirvish SS. Role of *N*-nitroso compounds (NOC) and *N*-nitrosation in etiology of gastric, esophageal, nasopharyngeal and bladder cancer and contribution to cancer of known exposures to NOC. Cancer Lett. 1995; 93: 17–48.

8 Dayal B, Ertel NH. Studies on *N*-nitroso bile acid amides in relation to their possible role in gastrointestinal cancer. Lipids. 1997; 32: 1331–40.

9 Puju S, Shuker DEG, Bishop WW, Falchuk KR, Tannenbaum SR, Thilly WG. Mutagenicity of *N*-nitroso bile acid conjugates in *Salmonella typhimurium* and diploid human lymphoblasts. Cancer Res. 1982; 42: 2601–4.

10 Busby WF Jr, Shuker DEG, Charnley G, Newberne PM, Tannenbaum SR, Wogan GN. Carcinogenicity in rats of the nitrosated bile acid conjugates *N*-nitrosoglycocholic acid and *N*-nitrosotaurocholic acid. Cancer Res. 1985; 45: 1367–71.

11 Totsuka Y, Nishigaki R, Enomoto S, Takamura-Enya T, Masumura K, Nohmi T, Kawahara N, Sugimura T, Wakabayashi K. Structures and biological properties of DNA adducts derived from *N*-nitroso bile acid conjugates. Chem Res Toxicol. 2005; 18: 1553–62.

12 Terasaki M, Totsuka Y, Nishimura K, Mukaisho KI, Chen KH, Hattori T, Takamura-Enya T, Sugimura T, Wakabayashi K. Detection of endogenous DNA adducts, O^6-carboxymethyl-2′-deoxyguanosine and 3-ethanesulfonic acid-2′-deoxycytidine, in the rat stomach after duodenal reflux. Cancer Sci. 2008; 99: 1741–6.

13 Kraemer KH, Seidman MM. Use of *supF*, an *Escherichia coli* tyrosine suppressor tRNA gene, as a mutagenic target in shuttle-vector plasmids. Mutat Res. 1989; 220: 61–72.

14 Yang JL, Chen RH, Maher VM, McCormick JJ. Kinds and location of mutations induced by (±)-7β,8α-dihydroxy-9α,10α-epoxy-7,8,9,10-tetrahydrobenzo[*a*]pyrene in the coding region of the hypoxanthine (guanine) phosphoribosyltransferase gene in diploid human fibroblasts. Carcinogenesis. 1991; 12: 71–5.

15 Matsuda T, Yagi T. Kawanishi M. Matsui S. Takebe H. Molecular analysis of mutations induced by 2-chloroacetaldehyde, the ultimate carcinogenic form of vinyl chloride, in human cells using shuttle vectors. Carcinogenesis. 1995; 16: 2389–94.

16 Girardi AJ, Jensen FC, Koprowski H. SV40-induced transformation of human diploid cells, crisis and recovery. J Cell Com Physiol. 1965; 65: 69–84.

17 Takebe H, Nii S, Ishii MI, Utsumi H. Comparative studies of host-cell reactivation, colony forming ability and excision repair after UV irradiation of xeroderma pigmentosum, normal human and some other mammalian cells. Mutat Res. 1974; 25: 383–90.

18 Akasaka S, Takimoto K, Yamamoto K. G, C to T, A and G, C to C, G transversions are the predominant spontaneous mutations in the *Escherichia coli supF* gene; an improved *lacZ-(am) E. coli* host designed for assaying pZ189 *supF* mutational specificity. Mol Gen Genet. 1992; 235: 173–8.

19 Seidman MM, Dixon K, Razzaque A, Zagursky R, Berman ML. A shuttle vector plasmid for studying carcinogen-induced point mutations in mammalian cells. Gene 1985; 38: 233–7.

20 Bubley GJ, Ashburner BP, Teicher BA. Spectrum of cis-diamminedichloroplatinum(II)-induced mutations in a shuttle vector propagated in human cells. Mol Carcinog. 1991; 4: 397–406.

21 Levy DD, Groopman JD, Lim SE, Seidman MM, Kraemer KH. Sequence specificity of aflatoxin B_1-induced mutations in a plasmid replicated in xeroderma pigmentosum and DNA repair proficient human cells. Cancer Res. 1992; 52: 5668–73.

22 Seidman MM, Bredberg A, Seetharam S, Kraemer KH. Multiple point mutations in a shuttle vector propagated in human cells: evidence for an error-prone DNA poly-

merase activity. Proc Natl Acad Sci USA. 1987; 84: 4944-8.

23 Courtemanche C, Anderson A. Multiple mutations in a shuttle vector modified by ultraviolet irradiation (±)-7,8-dihydroxy-9β,10α-epoxy 7,8,9,10-tetrahydrobenzo[a] pyrene and aflatoxin B_1 have different properties than single mutations and may be generated during translesion synthesis. Mutat Res. 1999; 430: 23-36.